TAMPEREEN TEKNILLINEN YLIOPISTO
TAMPERE UNIVERSITY OF TECHNOLOGY

JANNE HÄMÄLÄINEN

SEMI-CRYSTALLINE POLYOLEFINS IN FUSED DEPOSITION MODELING

Master of Science thesis

Examiners: Assistant Professor Essi Sarlin and Ilari Jönkkäri
Examiners and topic approved by the Faculty Council of Faculty of Engineering Sciences on 01.02.2017

ABSTRACT

JANNE HÄMÄLÄINEN: Semi-crystalline polyolefins in fused deposition modeling
Tampere University of Technology
Master of Science Thesis, 54 pages
September 2017
Master's Degree Programme in Materials Science
Major: Materials Science
Examiners: Assistant Professor Essi Sarlin and Ilari Jönkkäri

Keywords: polyolefin, polypropylene, polyethylene, fused deposition modeling, 3D printing, shrinkage, warping

With the continuous developments, FDM has surpassed the status as rapid prototyping method, and matured to the point where it is widely applied in direct manufacturing of various end-use products. However, the end-use applications are partly limited due to most current feedstock materials being prone to degradation in high-temperature, humid and chemically aggressive environments. The goal of this thesis was to evaluate the performance of polypropylene (PP) and polyethylene (PE) as alternative feedstock materials in the FDM process. PP and PE are prevalent polyolefin plastics and their principal value lies in the attractive balance of physical properties in the solid state and chemical inertness, and for the same reasons, they represent attractive FDM feedstock materials for the environmentally challenging conditions. However, as highly semi-crystalline plastics they show substantial solidification shrinkage upon cooling, and the shrinkage induced contractile stresses can deform the deposited parts.

In this work, the performance of PP and PE as feedstock materials in FDM was evaluated through several deposition experiments. The entire manufacturing chain from filament fabrication to deposition of specimens was controlled. Bonding quality between deposited filament strands at varying deposition conditions was assessed by preparing and testing tensile specimens, and comparing the results to injection molded counterparts. The effects of deposition conditions on the shrinkage and warp deformation were studied by depositing specimens with different geometrical features.

Based on the results, FDM of PP and PE feedstock materials is feasible and holds a great potential, but requires special arrangements and awareness of the inherent challenges. Bonding quality was highest at high temperature deposition conditions, and only roughly 10% loss in yield strength was observed when compared to injection molded counterparts. All specimens, regardless of deposition conditions, showed poor ductility and little to no correlation was found between the elongation and deposition temperatures. Excessive heat flow to the specimen during deposition caused substantial shrinkage due to prolonged cooling of the deposited plastic, and consequently the most dimensionally stable specimens were produced by limiting the deposition temperatures or increasing interlayer cooling time. Specimens with sharp protruding features showed higher tendency to peel off from the build platform than circular specimens did, due to differences in contractile stress distributions. Warp deformation became also more prominent when feature thickness was reduced. Nevertheless, the deposition performance under optimal conditions was for the most parts on par with many traditional feedstock materials.

TIIVISTELMÄ

JANNE HÄMÄLÄINEN: Osakiteiset polyolefiinit ekstruusiopohjaisessa 3D-tulostuksessa
Tampereen teknillinen yliopisto
Diplomityö, 54 sivua
Syyskuu 2017
Materiaalitekniikan diplomi-insinöörin tutkinto-ohjelma
Pääaine: Material science
Tarkastajat: Assistant Professor Essi Sarlin ja Ilari Jönkkäri

Avainsanat: polyolefiinit, polypropeeni, polyeteeni, 3D-tulostus, kutistuma, vääntymä

Vuosikymmeniä jatkuneen kehityksen tuloksena ekstruusiopohjaista 3D-tulostusta ei voida enää pitää ainoastaan pikamallinnusmenetelmänä. Teknologiana se on edennyt tasolle, jolla sitä voidaan hyödyntää niin yksittäisten lopullisten tuotteiden kuin pienten tuotantoerienkin valmistuksessa. Käyttökohteet ovat kuitenkin yhä rajalliset, sillä tulostusmateriaalien ominaisuudet usein heikkenevät kuumissa, kosteissa ja kemiallisesti agressiivisissa ympäristöissä. Tässä työssä tutkitaan polypropeenin (PP) ja polyeteenin (PE) suorituskykyä vaihtoehtoisina tulostusmateriaaleina. PP:n ja PE:n tasapaino kiinteän tilan fyysisten ominaisuuksien ja kemiallisen inerttiyden välillä on luonut pohjan niiden ylivoimaiselle valta-asemalle muiden muovien joukossa. Samoista syistä ne edustavat houkuttelevaa vaihtoehtoista tulostusmateriaalia vaativiin, lämpötiloiltaan vaihteleviin ja kemiallisesti agressiivisiin ympäristöihin. Osakiteisinä muoveina niiden kiteytymisprosessiin liittyvä kutistuma ja kutistumasta johtuva vääntyminen jäähtymisen aikana heikentävät kuitenkin tulostettujen kappaleiden mittatarkkuutta.

Tässä työssä kartoitettiin PP:n ja PE:n suorituskykyä vaihtoehtoisina tulostusmateriaaleina ekstruusiopohjaisessa 3D-tulostuksessa. Koko tuotantoketju filamentin valmistuksesta näytteiden tulostukseen oli kontrolloitu. Sulan filamentin sintrautumista eri tulostusolosuhteissa tutkittiin valmistamalla ja testaamalla vetokoenäytteitä, sekä vertaamalla tuloksia ruiskuvalettuihin kappaleisiin. Tulostusolosuhteiden vaikutusta kutistumaan ja vääntymään selvitettiin tulostamalla geometrioiltaan erilaisia kappaleita vaihtelevilla tulostusparametreillä.

Tulosten perusteella PP:n ja PE:n ekstruusiopohjaisessa 3D-tulostuksessa on potentiaalia, mutta prosessi vaatii erityisiä toimenpiteitä ja luontaisten haasteiden tuntemista. Suurin sintrauslujuus saavutettiin korkeimmilla tulostuslämpötiloilla, ja kappaleiden myötölujuus näissä olosuhteissa valmistettuna oli noin 90% ruiskuvalettujen kappaleiden arvoista. Venyvyys oli kuitenkin kaikilla kappaleilla heikkoa, ja sen korrelaatio tulostusolosuhteiden kanssa oli olematonta. Tulostuksen aikana liiallinen lämpövuo kappaleeseen aiheutti suuria kutistumia pitkittyneen jäähtymisen tuloksena. Mittatarkimmat kappaleet saatiinkin tulostettua rajoittamalla tulostuslämpötiloja tai pidentämällä kerrosten välistä jäähtymisaikaa. Erilaisten jäännösjännitysjakaumien takia kappaleet, joiden pohjassa oli teräviä ulkonemia, olivat alttiimpia irtoamaan tulostusalustasta tulostuksen aikana kuin pyörähdyssymmetriset kappaleet. Seinämäpaksuuksien ohetessa kutistumisesta aiheutuvat vääntymät tulivat myös paremmin esiin. Heikkouksistaan huolimatta, PP:n ja PE:n suorituskyky optimaalisissa tulostusolosuhteissa oli suurimmaksi osin verrattavissa moniin perinteisiin tulostusmateriaaleihin.

PREFACE

This thesis work has been conducted at the Department of Material Science of Tampere University of Technology in 2017.

I would like to thank my examiners Assistant Professor Essi Sarlin and Ilari Jönkkäri for their guidance throughout this work. They always provided unsolicited help with the practical aspects and experimental methodology of the thesis work. I would also like to thank my colleague, Tuire Marin, for her help and contribution in the experimental part, as well as for the encouraging peer support.

Of course, a warm thank you goes to my family and friends who have always been supportive during my years of studies, and this thesis work was no exception.

Tampere, 22.8.2017

Janne Hämäläinen

CONTENTS

LIST OF SYMBOLS AND ABBREVIATIONS

ABS	Acrylonitrile Butadiene Styrene
AM	Additive manufacturing
CAD	Computer aided design
CLTE	Coefficient of linear thermal expansion
CNC	Computer numerical control
DSC	Differential scanning calorimetry
FDM	Fused deposition modeling
HDPE	High-density Polyethylene
i-PP	Isotactic polypropylene
LC	Lumped capacity
LDPE	Low-density polyethylene
PA	Polyamide
PC	Polycarbonate
PCB	Printed circuit board
PE	Polyethylene
PEI	Polyetherimide
PETG	Polyethylene Terephthalate Glycol-modified
PLA	Polylactic Acid
PP	Polypropylene
PTFE	Polytetrafluoroethylene
RH	Relative humidity
RPM	Revolutions per minute
SLA	Stereolithography
SLS	Selective laser sintering
UHMWPE	Ultra-high-molecular-weight polyethylene

1. INTRODUCTION

The interest for fused deposition modeling (FDM) based additive manufacturing (AM) methods has grown enormously since the first applications in the late 1980s. With the expiration of the original patents, the increased accessibility has enabled easier adoption of this technology for both industrial and consumer level users. During the last three decades, FDM technology has in fact achieved a market leader position among the other plastics-based AM methods, such as selective laser sintering (SLS) and stereolithography (SLA) [1].

With the continuous developments in the field, the applications of fused deposition modeling are no longer limited to rapid prototyping purposes only. As a technology, FDM has matured to the point, where it can be employed in various end-use applications and direct manufacturing of limited product series on demand. Although the range of available materials is constantly expanding, some limitations in the field still exists, due to many feedstock materials being prone to degradation in harsh environmental conditions. High temperature, humidity and chemically aggressive environments can impair the functionality and aesthetics of parts prepared via fused deposition modeling. Further developments in feedstock materials are thus needed to allow FDM technology to reach its full potential in the wide area of end-use applications.

This work was conducted to evaluate the performance of polyolefin materials as feedstock materials in FDM process. Polyolefins are a group of polymers produced through the polymerization of simple olefin (also known as alkene) molecules. The most prevalent polyolefins are polypropylene (PP) and polyethylene (PE), which can be found nowadays in a wide array of applications. The principal value of these materials lies in their attractive balance of physical properties in the solid state and their superior chemical resistance. With these attributes, they also represent an appealing option as alternative FDM feedstock materials for environmentally challenging conditions, expanding the applicability of FDM. However, semi-crystalline polyolefins suffer from high solidification shrinkage upon cooling due to the transition from low-density amorphous form to ordered high-density state. The contractile forces arising from the shrinkage can induce warp deformation, impairing the functionality and aesthetics of the deposited articles.

Very little research been done on the performance of polyolefins as feedstock materials in FDM. Although a few studies have briefly assessed the topic [2-4], no comprehensive performance evaluation has been carried out to date. The literature review in this thesis provides considerations on the potential and feasibility of polypropylene and polyeth-

ylene as alternative feedstock materials. In the experimental section, the deposition performance is assessed by depositing several test specimens with varying geometries to evaluate the bonding, shrinking and warping characteristics of these materials in the FDM process. The overall deposition performance and suggestions for further research will be discussed in the finishing chapters.

2. THE CONCEPT OF FDM

Fused deposition modeling, also commonly referred as extrusion based 3D printing, is an additive manufacturing (AM) technique in which a 3D physical object is created directly from a digital computer-aided design (CAD) model. The objects are deposited layer-by-layer on a build surface, typically by liquefying and extruding amorphous thermoplastic polymer filament through a small nozzle. The extruding components move along perpendicular axes according to predefined computer numerical control (CNC) commands, while depositing the 'roads' of polymer. The 3D object is gradually constructed, as the roads are repeatedly deposited and solidified. [1]

One of the distinctive benefits of FDM is the ability to fabricate products with complex geometries that would be impossible or very challenging to implement with conventional techniques [5, 6]. The possibility to control the internal structure of components during the building has enabled various innovations in many engineering fields. The intermediate manufacturing steps between a CAD model and a finished product, such as mold manufacturing in injection and compression molding, are also unnecessary when using additive manufacturing methods. For prototyping and low volume production purposes, this implies significant economic advantages, and the general interest has consequently grown enormously since the filing of the early patents by Stratasys in the late 1980s [7]. With the recent expiration of original patents relating to FDM, the increased accessibility has enabled easier adoption of this technology for both industrial and consumer level users [8, 9]. During the last three decades, FDM technology has in fact achieved the market leader position among the other plastics-based AM methods, such as selective laser sintering (SLS) and stereolithography (SLA), and further growth is expected in the future [1, 10, 11].

The purpose of this chapter is to give reader a sufficient understanding of the principles behind fused deposition modeling process to recognize the challenges in FDM of polyolefin based materials. This includes the practical procedure of FDM, the critical parameters governing the bonding of polymer roads, as well as the range and properties of the conventional feedstock materials that are available at the time of writing of this thesis. The challenges of polyolefin based filaments as FDM feedstock material candidates will be addressed from a material scientific standpoint in later chapters.

2.1 The FDM process and general tool chain

In fused deposition modeling process, 3D physical objects are directly manufactured according to a CAD model. This direct manufacturing method reduces the amount of steps

that are present in conventional plastic product manufacturing, into a very straightforward and brief process chain.

The whole FDM procedure breaks down into four general stages [12]:

1. Modeling in CAD software.
2. Setting process parameters in FDM software.
3. Deposition of the physical 3D object.
4. Post processing.

As for most additive manufacturing processes nowadays, the fabrication begins with the design of a digital 3D CAD model of the part in development. A large range of commercial, as well as open source and freeware solutions are available for this step in the process chain [13]. However, typically the CAD model in itself is not enough for FDM purposes. Conventionally the CAD files are converted into stereo lithography format (STL), which transforms the design into a closed surface representation of the original model [14]. The STL file is further processed in FDM software, which slices the geometry into thin cross-profile layers and calculates the path for the extruding components. Nearly all additive manufacturing machines readily accept the sliced STL file format and print according to generated tool path created in the FDM software. [1, 14].

Before feeding the STL file to the fused deposition modeling machine and printing the object, the critical parameters governing the deposition and bonding of the individual polymer roads need to be decided. Most industrial machines allow the modification of key parameters in FDM software, so that the fabrication process can be optimized for any given filament material and component. Most important hardware related parameters defining the quality of a deposited object are deposition temperature, deposition speed and part cooling. Some FDM machines have heated build platforms or heated build chambers, which allow a more refined control over the cooling characteristics of the deposited polymer roads. Slicing parameters, such as layer height, infill amount and pattern, extrusion orientation and raster angle also have a great impact on the dimensional accuracy and mechanical properties of the fabricated parts. [5, 15] Operator of the fused deposition modeling machine needs to have a proper understanding of the aforementioned parameters and their effect on the final print quality for best results. Thus, the key variables will be further discussed in Chapter 2.2.

Once the important parameters are set, the FDM machine carries out the actual building of the physical 3D object. Main elements in any melt extrusion based additive manufacturing machine are print head with liquefier, material feed mechanism and build surface [11]. Figure 1 shows a schematic representation of a typical print head setup with a feed mechanism. The print head itself usually moves in horizontal X-Y plane while depositing polymer roads on the build surface moving along vertical Z plane [1, 16]. A wide range

of different solutions for moving the print head and build surface are available, most of which work in Cartesian coordinate system. Motor driven roller mechanism feeds the filament into the print head, in which the liquefier, sometimes referred as hot end, melts and deposits it on the build surface. Heat flux from the liquefier to the feedstock material affects the viscosity of the polymer melt, and thus the pressure drop in the nozzle and the overall deposition rate. As a result, extrusion temperature and rate settings need careful consideration and their correlation should be taken into account when setting process parameters [17].

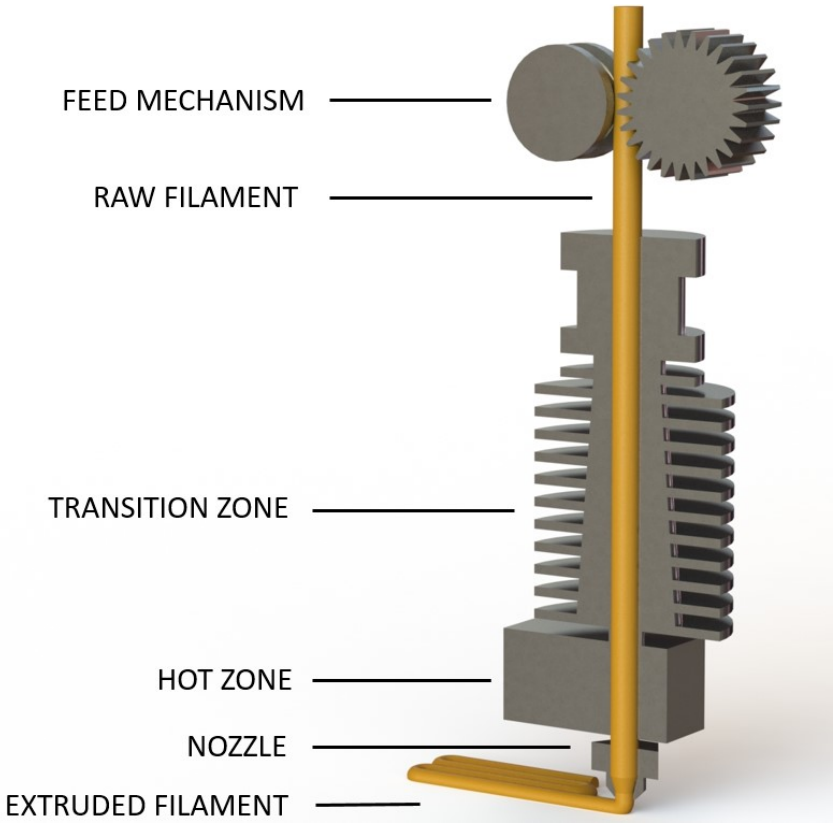

Figure 1. *A schematic representation of a typical print head with extrusion mechanism. Motor driven roller mechanism feeds the filament to the print head, which liquefies and deposits the polymer on the build surface.*

Eventually, a physical 3D object analogous to the digital model builds up on the build surface. Depending on the part and its end-use application, some post-processing may be needed. To achieve proper fit and function, accuracy improvements and property enhancements may be required. Different surface texture improvement methods can attenuate the layered appearance characteristic to fused deposition modeled parts and give a finish closer to molded products. Wide range of accuracy, aesthetic and property enhancement methods have been researched and introduced in literature, including solution treatments, vapor smoothing with solvents, resin infiltration and coatings. [10, 18-22]

2.2 Critical process variables

2.2.1 Categorization of process variables

The quality of a fused deposition modeled part is greatly affected by the selection of suitable process variable values for any chosen filament material. Although the basic working principles of FDM are fairly straightforward, the complexity of polymer melt dynamics, cooling characteristics and bonding processes during deposition complicates the selection of appropriate parameter values. A few build iterations may be needed before the optimal settings are established.

The key variables in FDM process can be divided into operation specific and build strategy specific categories. Table 1 lists the key variables used in fused deposition modeling. User typically has control over operation specific variables, such as extrusion temperature, extrusion flow rate and print head speed. Depending on the machine, temperature of heated build platform and build chamber may also be adjustable. Build strategy specific variables are set in FDM software and essentially define the toolpath for the print head. Build strategy related variables include layer height, deposition orientation, infill pattern, infill amount and raster angle. A big influence of these parameters to the mechanical properties and anisotropy has been show in several studies [2, 23, 24].

Table 1. *Key deposition variables divided into operation and build strategy specific categories.*

Operation specific	Build strategy specific
Extrusion temperature	Layer height
Heated platform temperature	Infill amount
Heated chamber temperature	Infill pattern
Extrusion flow rate	Raster angle
Print head speed	Deposition orientation

The effects of most of these variables have been thoroughly investigated. However, the majority of the research focuses on common FDM plastics, such as acrylonitrile butadiene styrene (ABS) and polylactic acid (PLA), whereas more novel materials have been of low interest. Therefore, more research is needed to gain better understanding and predictability of wider range of the materials available for FDM.

2.2.2 Operation specific process variables

When it comes to melt extrusion based manufacturing methods, the extrusion temperature is arguably the single most important variable that affects the quality of deposited parts. The melt dynamics, cooling characteristics and bonding processes during deposition are

all dependent on the selection of this parameter, and thus finding the most suitable value is vital for good results. The adjustment of extrusion temperature is based on the controlling of heat flux from the liquefier to the feedstock material. Heat flux should be high enough to bring the feedstock material in to a readily flowing state but low enough to prevent unwanted oozing and thermal degradation of the polymer during extrusion [11]. Typically, the liquefier temperature ranges from 180 °C to 280 °C, depending on the glass transition (T_g) and melting temperatures of the feedstock material [25].

The bonding of deposited polymer roads is driven by the thermal energy of the extruded filament. The neck formation, molecular diffusion and randomization at the interface between the adjacent roads are the main mechanisms affecting the bond quality. Figure 2 shows a schematic representation of the neck formation between two adjacent polymer roads. Generally, higher extrusion temperatures allow better necking and molecular diffusion at the interface and thus better overall mechanical properties. Sometimes the term 'sintering' is also used to describe the necking of polymer roads above their glass transition and melting temperatures. This can be misleading, as sintering is typically defined as coalescence below melting point. However, the term 'sintering' has been widely accepted and used in the literature for describing the coalescence of polymers also above the glass transition and melting temperatures [26].

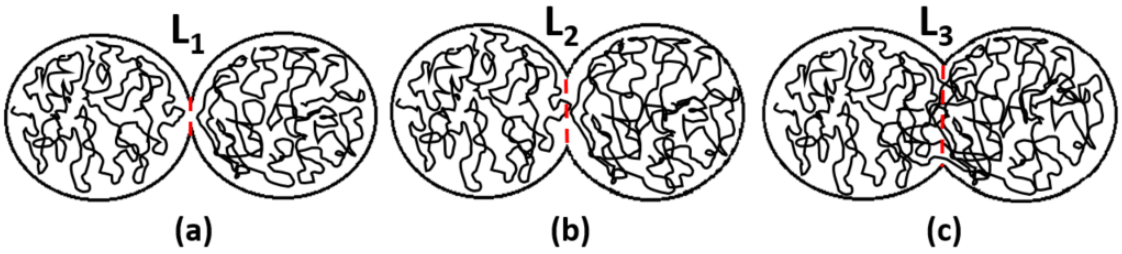

Figure 2. *Neck formation and molecular diffusion at the interface between adjacent polymer roads at T_1 (a), T_2 (b) and T_3 (c).*

In addition to extrusion temperature, the temperature history of the deposited filament is of major importance for the bond quality. The temperature history depends on the cooling conditions of the deposited polymer road once it leaves the liquefier nozzle. Besides the bond quality, the cooling conditions dictate the shrinkage and potential dimensional distortion of the deposited parts. Shrinkage and distortion issues will be addressed in more detail in Section 3.3.

The heat transfer dynamics surrounding the cooling of deposited polymer roads are complex and little research has been done in order to gain a better understanding and predictability of this phenomenon. One of the earliest studies on the subject by Rodriguez (1999) focused on a transient 2D analysis of the heat transfer in FDM via finite element method [27]. Later Thomas *et al.* (2000) developed a heat transfer model, where the cross sections

of polymer roads were idealized as rectangles and perfect contact between roads was assumed [28]. Model suggested that cross sectional temperature gradients in the filament are negligible once the consecutive road is deposited above. Based on these results, Li *et al.* developed a model for cooling process using lumped capacity (LC) analysis and by simplifying the model into one-dimensional heat transfer model [29]. Above heat transfer models have been validated by Sun *et al.* by experimental work, using ABS plastic and monitoring the temperature profiles of deposited roads with thermocouples. Figure 3 shows the comparison between the experimental data and analytical models. The measured data seemed to be in general agreement with the theoretical models. However, the 2D analytical model seemed to be more accurate at lower temperatures and longer times, whereas the LC model was in better agreement with experimental date at high temperatures and shorter times. [26]

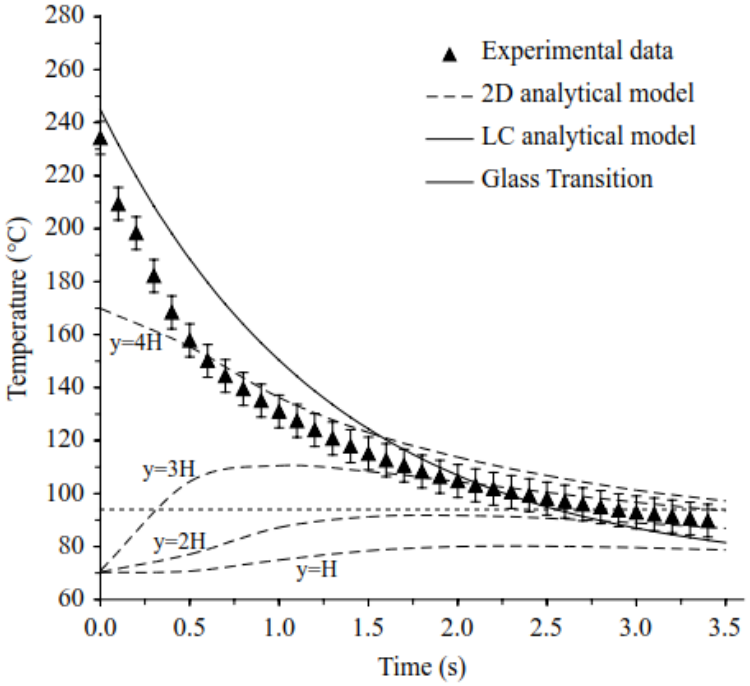

Figure 3. *Validation of heat transfer models by Sun et al. Curves represent the cooling of polymer road once it has left the nozzle. Dashed lines denote the predictions of 2D analytical model at layer number H. Experimental data was gathered using ABS plastic. [26]*

After the deposition, the time above glass transition temperature, T_g, is very short and most of the sintering takes place during this time period. Some studies have suggested that most of the sintering occurs above a critical sintering temperature, which can be significantly higher than T_g. According to Bellehumeur *et al.* [30] and Li *et al.* [31] the critical sintering temperature of ABS P400 plastic is as high as 200 °C, whereas the T_g of the plastic is only 94 °C.

Cooling characteristics of the polymer road are of course also dependent on the speed at which the print head moves while depositing filament. The faster the print head moves, the less time the already deposited road has to cool down before a successive molten road is deposited above. User typically has control over both printing and travel speeds. Printing speed is the speed at which the print head moves while depositing the filament, whereas the travel speed is defined as the speed only used for travel moves between disconnected points in tool paths without depositing filament. Decreasing either of these speeds increases the layer cooling time. The cooling characteristics of the deposited polymer can be thus modified by adjusting the speed settings or printing multiple components in the same print run.

As FDM-based machines have become more affordable, even the most consumer level machines now have an option to heat up the build platform to control the cooling and adhesion during printing. With sufficient power supply, these heated platforms are capable of reaching 180 °C, which is more than enough for the available feedstock materials [2]. As the filament is deposited layer by layer on the build surface to create a physical 3D object, significant thermal gradients are always present. Large thermal gradients will typically lead to dimensional distortion, as the temperature and shrinking rates during cooling differ between various areas of the part. Heated build platform reduces the thermal gradients in the part during deposition and consequently decreases the possibility of unwanted distortions [11].

Heated build platform will also affect the sintering process of the polymer roads. Even though most of the sintering occurs above critical sintering temperature [30, 31], the additional heat from the heated build platform slows down the cooling and facilitates the neck formation to some extent. The additional heat and increased time above T_g in the bottom part of the object leads to situation in which the neck growth in the lower layers of the part is higher than in the top layers, as shown in Figure 4.

Industrial FDM systems commonly have a heated build chamber for more accurate control of cooling conditions. These chambers heat up and circulate enclosed air, and typically work at temperatures below 100 °C. The reduction of thermal gradients and potential distortions in the deposited part is more uniform than in the case of heated build platform.

Prior research has shown that the difference in neck radius in the bottom and top layers is substantial, and can be as high as 50% over 30 layers of deposited polymer when using a heated build envelope [26]. Although the difference in neck growth along vertical axis admittedly causes variation in mechanical properties, for some feedstock materials the heated build envelope is necessary to avoid dimensional distortion. The effects of heated build platform and build envelope will be further discussed in Section 3.3.

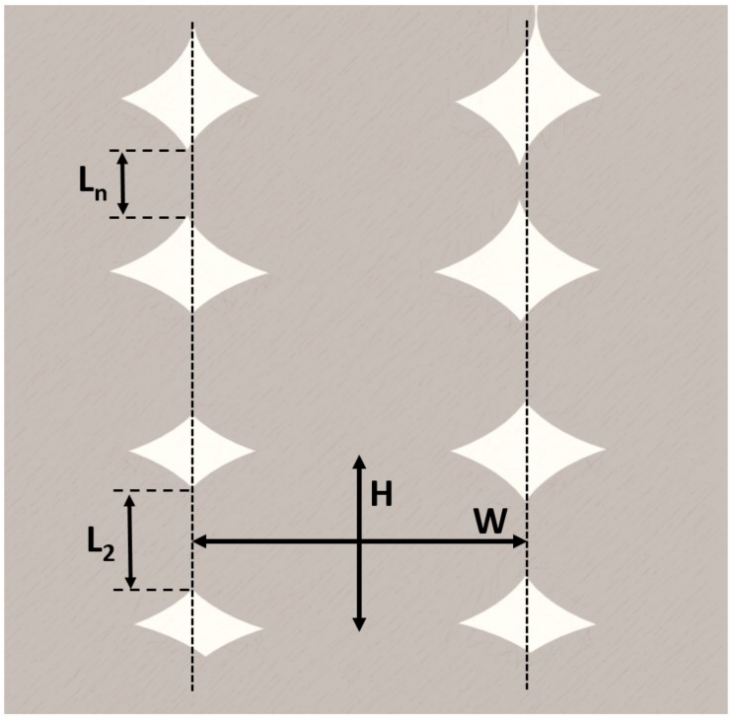

Figure 4. *Growth of neck length ($L_2 > L_n$) between adjacent filaments towards bottom layers due to the additional heat from heated build platform and chamber.*

The final important operation specific process variable is the extrusion flow rate. Typically, FDM software automatically calculates the correct flow rate based on the filament diameter and print head speed to ensure sufficient extrusion at all times. However, user can adjust the flow rate manually to fine tune the necking behavior of adjacent polymer roads. By increasing the extrusion multiplier, more filament is fed through the nozzle than the automatically calculated value suggests. This leads to more squashed roads and increased necking, which in turn reduces porosity and can improve mechanical properties of the deposited component. Over extrusion, however, should be avoided since it can lead to dimensional inaccuracy and aesthetic issues. By decreasing the extrusion multiplier, less filament is fed through the nozzle and individual polymer roads are more clearly separated. Under extrusion can thus inhibit sufficient necking and severely impair mechanical properties.

2.2.3 Build strategy specific process variables

Build strategy specific process variables essentially define the toolpath, which the print head follows while depositing filament. These variables show clear correlation with final mechanical properties of the part and should be carefully set, in order to achieve the optimal strength for a specific application. Most of the variables also affect the build time, which should not be excluded from the optimization process.

Layer height defines the length of the discrete step, which the print head moves in relation to build platform in vertical direction between layers. Typical layer heights range from tens of micrometers up to one millimeter, depending on the size of the nozzle. Larger diameter nozzles can extrude more polymer per time unit and are thus able to deposit at higher layer heights. Due to the layer-by-layer building technique, the layer height is a critical variable defining the quality of surface finish as well as the build time [32].

One of the most characteristic features of FDM is the ability to control the inner structures of the deposited part. While conventional manufacturing methods are usually restricted to using solid material infill for all areas in the part, FDM allows the control of the amount and type of infill within enclosed structures. This permits the optimization of strength-weight relationship in a novel and efficient manner [33]. The amount of infill is a major factor defining the mechanical strength of the final part, higher infill percent providing better strength. Carneiro *et al.* observed over 250% differences in modulus and strength when changing the infill amount from 20% to 100% [2]. The lower limit of infill is restricted by its ability to support the successive layers without adversely affecting the deposition, and normally at least 10% of volumetric infill is needed. For any load-bearing purposes, a higher infill percent should be considered. The type of infill can range from simple raster pattern to honeycomb structure, depending on the slicing software. Figure 5 shows some common infill patterns at 20% infill amount available in Slic3r Prusa Edition 1.34.1 open-source slicing software. A number of perimeter layers confines the infill portion in order to provide a clean and continuous external surface.

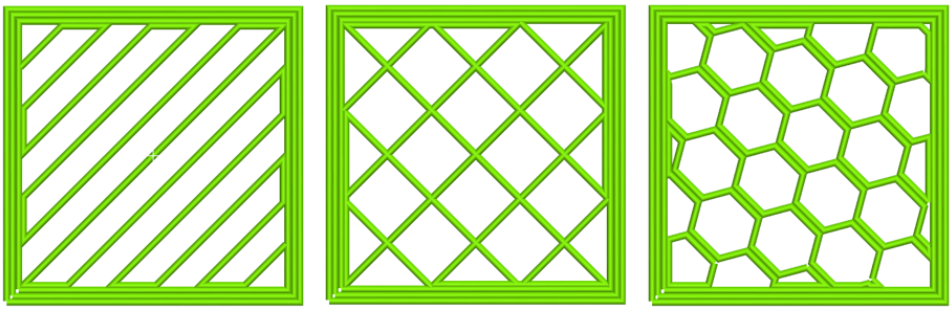

Figure 5. *Common infill patterns at 20% infill amount available in Slic3r Prusa Edition 1.34.1 open-source sclicing software: (a) rectilinear raster, (b) grid, and (c) honeycomb.*

Raster angle of the infill also affects the structural properties of the final part, and should be set with respect to end-use applications. While crossed 45° raster is a common choice for infill, for pure tensile strength purposes, infill raster parallel to tensile stresses yields the highest tensile strength. Aligning the deposition orientation with the applied stress minimizes the problems related to adhesion between filaments, since the interfaces are not subjected to tensile forces. [2]

One final thing to consider is the part deposition orientation. Orientation refers to the inclination of part within the build envelope with respect to the printer axes [34]. A lot of research has been done in order to optimize the part building orientation for different objectives like dimensional accuracy, mechanical properties and build time [35-38]. General rule of thumb is to avoid tensile stresses across the filament interfaces to minimize the problems related to adhesion, and orient the part accordingly in the slicing software.

2.3 Common feedstock materials

Although the range of different feedstock materials for FDM is vast, both consumer level and industrial machines primarily utilize a few mainly amorphous thermoplastic materials. These materials tend to have low coefficient of linear thermal expansion (CLTE) and low solidification shrinkage upon cooling, which reduces distortions in the finished part. On the other hand, many traditional feedstock materials are relatively brittle, prone to degradation in chemically aggressive environments, and practical temperature range for applications is often limited.

Due to the increasingly growing interest towards FDM, the research for better feedstock materials has been very active [1]. Since the availability and adoption of open-source FDM machines has grown, users are no longer limited to proprietary materials, which in turn has created a market for novel materials.

Various acrylonitrile butadiene styrene (ABS) and polylactic acid (PLA) based filaments are predominant in industrial and consumer level machines. While various ABS based plastics have traditionally been used in industrial FDM applications, PLA has gained popularity among users with personal desktop machines for its easy printability and good mechanical properties [39].

ABS is an amorphous thermoplastic polymer with glass transition temperature of approximately 100 °C and maximum CLTE of around 15×10^{-5}/°C, depending on the grade [39]. The common extrusion temperatures for different ABS grades range from 230 °C to 270 °C [40-42]. Shrinkage values between 0.7% and 1.6% have been reported [39]. Although being an amorphous polymer and showing lower shrinkage than most semi-crystalline polymers, ABS typically requires a heated build platform and a build envelope for a successful print, due to its tendency to warp slightly during printing. Usually bed temperatures between 100 °C and 120 °C [40, 43] and build envelope temperatures between 50 °C and 70 °C are used [26]. ABS products have intrinsically high strength and decent corrosion resistance at fairly low price, allowing manufacturing of products for numerous end-use applications [44]. A wide range of different ABS grades is available for FDM purposes with tailored properties for varying applications [1].

PLA is a biodegradable semi-crystalline thermoplastic polymer produced from renewable resources, such as sugarcane or corn. Despite of being a semi-crystalline polymer, it has

a wide melting range, extending from its T_g of around 60 °C to the melting temperatures of the crystalline parts at 150-180 °C [39]. PLA has a slow crystallization rate, and consequently has not been extensively used in injection molding. Obtaining highly crystalline PLA in injection molding would require slow cooling rates, leading to long cooling times and inefficient process [45]. However, for FDM purposes PLA is a well-fitting material due to its low shrinkage and low CLTE of 8.5×10^{-5}/°C [39]. Annealing PLA above its T_g improves mechanical properties and temperature resistance due to increased crystalline content. This process has been studied for both injection molded and 3D printed PLA [39, 45]. The extrusion temperature for PLA in FDM ranges from 180 °C to 220 °C, depending on the grade. Since only minimal shrinkage is present during printing, heated build platforms or envelopes are not required. The adhesion to the print bed can be improved by using common adhesives such as glue sticks and hair spray, or blue painters tape. [39]

Although most of the past and ongoing research focuses on feedstock materials based on above polymers, the interest in entirely new filament materials is growing. Many FDM machine manufacturers have started to branch out into new materials, and proprietary feedstock selection is no longer limited to only few common polymers. Several high performance feedstock materials, such as polycarbonate (PC), polyetherimide (PEI), glycol modified polyethylene terephthalate (PETG) and polyamide (PA) have been researched and are available in filament form for FDM purposes [1, 44, 46-48]. Blends between some of the aforementioned materials have also been studied with good results [49, 50]. Filling polymer matrices with metallic or ceramic particles and fibers has shown promising results as well [51-54].

3. POLYOLEFINS IN FDM

Despite of the recent developments, the spectrum of available FDM filaments is still rather limited, preventing the technology from reaching its full potential. In this work, the potential and feasibility of the two most common polyolefins, namely polypropylene and polyethylene, as FDM feedstock material candidates will be evaluated. These two commodity plastics have a good overall balance between mechanical, physical and chemical properties, and come at substantially lower cost than most of current FDM feedstock materials. PP and PE are also very versatile materials and can be tailored for various applications and manufacturing processes. [57] The unique balance between the properties of these materials represents an attractive possibility to extend the applicability of FDM for even wider range of products. Sections 3.1 through 3.4 will address the benefits of adapting PP and PE into the FDM process, as well as the inherent challenges that they will introduce to the process.

Polyolefins are a group of thermoplastic polymers produced by the polymerization of simple olefins such as ethylene, propylene or isoprenes. These olefins are commonly obtained from natural carbon sources, including crude oil and gas. The polymerization process and the type of monomer are the key factors influencing the molar mass and degree of crystallinity, essentially defining the properties of the polymer [56]. Generally, polyolefins offer an attractive set of mechanical and physical properties at very low price, which has made them the most produced plastics of all time. In 2015, the production of polypropylene and polyethylene reached 177,5 million tons, and the production of PE alone is expected to reach 100 million tons in 2018 [56].

Polypropylene is a thermoplastic polymer produced by polymerizing propylene molecules (C_3H_6) into long chains. Catalysts for the polymerizing reaction are typically chosen so that the process yields crystallizable isotactic PP (i-PP) [57]. Most PP grades tend to be semi-crystalline, i.e. their morphology contains both crystalline and amorphous phases. The relative amount of these phases depends on the stereochemical and structural characteristics of the chains, as well as the processing conditions during the final manufacturing of products. During the cooling from melt, a spherulitic crystalline morphology develops in PP, and the crystallization temperature, as well as the spherulite size, can be modified by adding nucleating agents. The melting temperature of PP homopolymer lies at around 160 °C, while typical PP random copolymers melt around 145 °C. The glass transition temperature of amorphous parts in isotactic PP is difficult to detect accurately due to the high crystalline-amorphous ratio. However, atactic PP grades show a clear glass transition at around -15 °C. PP has excellent mechanical, physical and thermal properties for many relatively low temperature applications, while allowing easy modification of these properties by altering the chain regularity. [57, 58]

Polyethylene is the single most used thermoplastic polymer around the world, taking over 31% share of the global plastic market [56]. It is produced by polymerizing ethylene molecules (C_2H_4) into long polymer chains and the polymerization process essentially defines the length and amount of branching in PE molecules. Traditionally, PE is classified as having either low (LDPE), medium or high (HDPE) density, depending on the level of branching. In HDPE, the amount of branching is low or virtually nonexistent, allowing the polymer to crystallize effectively into a high-density ordered state. On the other hand, LDPE contains a substantial concentration of branches and other chain defects that hinder the crystallization and increase the amount of amorphous portion in the morphology. The density of PE varies from 0.90 g/cm^3 of LDPE to 0.97g/cm^3 of HDPE. The melting point of HDPE lies around 130 °C, but decreases to 100 °C of LDPE, as the amount of chain irregularities increases. The glass transition temperature of polyethylene ranges from -20 °C to -140 °C, depending on the grade. Thus, PE remains in a ductile state virtually in all commercial applications. [59] The CLTE of PE varies between 12×10^{-5}/°C and 20×10^{-5}/°C, and mold shrinkage values up to 3.0% have been reported [60]. For FDM purposes, HDPE is the most interesting candidate due to its impact strength, low permeability and good corrosion resistance. Based on these attributes, it has been widely adopted in water, sewer and natural gas transportation applications, for example. However, the high shrinkage of PE challenges the FDM process.

3.1 Benefits of polyolefin based filaments

3.1.1 Chemical and environmental resistance

On a general level, polyolefins exhibit exceptionally high chemical resistance compared to many other commodity plastics. Both PP and PE are resistant to different non-oxidizing acids, aqueous salt solutions, aqueous alkalis and polar solvents [61, 62]. However, PP and PE absorb non-polar solvents, such as chlorinated solvents and hydrocarbons more readily than polar solvents. PP and PE are also attacked by oxidizing agents, such as nitric and sulfuric acids, and halogens. PP is generally more prone to oxidizing agents due to the tertiary hydrogen atoms compared to the PE with only secondary hydrogen atoms. [60, 63, 64]

Despite of the few minor limitations, PP and PE are excellent materials for applications involving mixtures of acids, bases and solvents, such as industrial and laboratory drainage piping. The high chemical resistance opens up new possibilities in the area of FDM, as many of the current feedstock materials are more prone to the corrosive effects of these chemicals and have thus limited the range of feasible applications of FDM [65]. The possibility to produce chemically and environmentally inert articles based on a digital model within hours is an attractive scenario for many industrial areas.

3.1.2 Low water and moisture absorption

Moisture absorption of FDM feedstock materials imposes serious issues for the quality of the processed parts. When filament with absorbed moisture is extruded through the liquefier, the water in the material vaporizes and forms voids in the deposited polymer. The internal voids decrease the mechanical properties of the finished part and can deteriorate the surface finish. Additionally, the absorbed moisture can break down polymer chains through hydrolysis, degrading the material.

One of the benefits of polyolefin based FDM feedstock materials is their inherently low water absorption. The water absorption of PP and PE is in fact an order of magnitude lower than in some common feedstock materials (see Table 2). Whereas other feedstock materials may require special storage conditions and thorough drying process prior to deposition, PP and PE can be deposited right after storing in ambient conditions. This can impose substantial economic savings for the process, as drying FDM feedstock materials in an oven or vacuum with desiccant can be costly.

Table 2. *Comparison of water and moisture absorption between common raw FDM feedstock materials. Data adapted from [62].*

Material	Water Absorption at 23 °C (%)	Moisture Absorption at 23 °C / 50% RH (%)
High Density Polyethylene (HDPE)	0.005-0.01	-
Polypropylene (PP)	0.02-0.04	-
Polyethylene Terephthalate (PET)	0.04-0.6	0.035
Polycarbonate (PC)	0.12-0.40	0.09-0.3
Polylactic Acid (PLA)	0.5	3.9
Polyetherimide (PEI)	0.65-1.75	0.15-0.76
Acylonitrile Butadiene Styrene (ABS)	0.7-1.03	0.21-0.35
Polyamide-12 (PA-12)	0.8-1.5	0.4-0.8
Polyamide-6.6 (PA-6.6)	4.7-9.0	1.4-3.4

While the low water absorption is beneficial to the FDM process itself, it also allows the fabrication of articles for end-use applications where the finished parts are imposed to humid conditions. These applications include drainage piping and other liquid transporting areas, for example. The use of conventional FDM feedstock materials under such conditions may not be feasible due to excessive swelling and degradation. [66-68]

3.1.3 Mechanical properties

The principal value of polyolefins lies in their attractive balance of chemical inertness and physical properties in the solid state. Semi-crystalline PP and PE possess a combination of relatively high stiffness, strength and toughness while being among the lightest

commercial plastics [56]. This set of properties is not commonly found in FDM feedstock materials, making PP and PE attractive and unique feedstock candidates for the process. A set of mechanical properties of polyolefins and other polymers are compared in Table 3. Although some common FDM feedstock materials show higher mechanical performance, the performance may reduce when exposed to weathering or corrosive conditions. Under such conditions, polyolefins are able to retain their mechanical properties better due to chemical inertness.

Table 3. *Comparison of mechanical properties between some typical raw FDM feedstock materials. Data adapted from [62].*

Material	Density at 20 °C (g/cm^3)	Tensile Strength (MPa)	Elongation (%)	Young's Modulus (MPa)
High Density Polyethylene (HDPE)	0.94-1	13-51	250-1200	800
Polypropylene (PP)	0.84-0.91	26-32	10-140	1200-2000
Polyethylene Terephthalate (PET)	1.3-1.4	24-41.4	100-250	2000-2700
Polycarbonate (PC)	1.19-1.22	55-88	66-140	2390-2600
Polylactic Acid (PLA)	1.21-1.29	52-72	4-6	3700-4100
Polyetherimide (PEI)	1.27-1.31	53-124	14-50	3000
Acylonitrile Butadiene Styrene (ABS)	1.03-1.09	25-65	8-20	2300
Polyamide-12 (PA-12)	1.01-1.03	50-70	<50	460-1900
Polyamide-6.6 (PA-6.6)	1.05-1.14	70-88	10-45	173-508

The mechanical properties of polyolefins are also highly customizable, making it easy to tailor them for many specific applications. By modifying the chain structure, e.g. branching and tacticity of the backbone, the degree of crystallization can be controlled. Increased degree of crystallization typically shows as increased density, strength and stiffness.

3.1.4 Availability of materials and economic impacts

Due to a strong competition between various plastic construction and engineering materials, the development of cost-effective materials is constantly ongoing and expanding. During the last few decades, polyolefin materials have gained a well-established position among these materials, and even larger growth is expected in the future. This notable development is attributed to the ease of polyolefin production from a variety of sources, cost-effectiveness, and the unique balance of physical properties and chemical inertness [57].

The raw material prices of common polyolefins, such as PP and PE, are currently among the lowest of all plastic materials [69, 70]. The cost of raw feedstock materials used in

FDM process is a noteworthy factor to consider, especially if high performance engineering plastics are used and products are manufactured in large quantities. Competitively priced polyolefins could thus gain a position as a cost-effective replacement of many engineering plastics, and allow easier adoption of FDM technique for many industrial areas.

3.2 Adhesion properties of polyolefins

Polyolefins exhibit an excellent balance of properties for numerous applications. However, a common issue for most polyolefins are poor surface adhesion properties. Low adhesion represents a serious problem when coating or laminating polyolefins with other materials, and insufficient adhesion leads to delamination between the polyolefin substrate and the coating.

A common reason for poor adhesion is a contaminated surface. Contaminants should be removed before joining for example, by solvent wiping. In the case of polyolefins, solvent wiping alone is typically not enough to ensure an effective adhesion between two surfaces. Polyolefins have inherently low surface free energy, low polarity, and they lack functional groups on the surface, resulting in poor intrinsic adhesion [56, 71]. Various surface modification methods in packing, automobile and building industries are thus used to improve the adhesion to sufficient level for coating purposes. Common methods include chemical modification and plasma or corona treatments. The aim of these treatments is to create functional groups at the interface of the two material surfaces to increase the surface polarity. Increased polarity improves the adhesion strength by increasing the molecular forces between the two surfaces. [71]

In fused deposition modeling, the adhesion properties of feedstock materials are also a major factor to consider. The sufficient adhesion between the first layer and the build platform, as well as the self-bonding of the polymer during building is critical for the success of the deposition. For common feedstock materials, e.g., ABS, PLA, and PETG, several different adhesives and adhesion promoting build surfaces are available. However, the adhesion of polyolefins to even these surfaces is insufficient, which imposes a challenge for the whole FDM process. Previously discussed adhesion promotion treatments are generally not feasible for FDM use, and typically self-bonding between the first layer and build platform is needed, i.e., using the same feedstock material also as build platform material [2, 4, 72]. The adhesion to build platform is especially important in the case of semi-crystalline feedstock materials, as the shrinkage during cooling can cause warping of the deposited object and eventually lead to partial or complete delamination from the platform. The shrinkage and shrinkage induced warping will be discussed in more detail in following chapters.

3.3 Dimensional stability

3.3.1 Shrinkage of semi-crystalline polyolefins in FDM

In general, polymers show greater correlation between specific volume and temperature than metals or ceramics. Both amorphous and semi-crystalline polymers show substantial linear thermal expansion upon heating. In addition to linear thermal expansion, semi-crystalline polymers display a large change in specific volume around melting temperature (T_m) due to crystallization phenomenon. It is the net effect of both linear volumetric shrinkage and crystallization shrinkage that dictates the total shrinkage of semi-crystalline polymers upon cooling. As highly semi-crystalline polyolefins, both PP and HDPE suffer from the temperature related dimensional instability. The combination of thermal gradients and shrinkage upon cooling generates contractile forces between the deposited layers, and can eventually lead to warp deformation. This chapter provides discussion on the relationship between the degree of crystallization and FDM process parameters in order to recognize the origins for the dimensional instability.

Although completely amorphous polymers do not go through a first order phase transition, the coefficient of linear thermal expansion increases slightly around the glass transition temperature upon heating. The morphology remains virtually unchanged while the polymer transforms from rigid glassy state to rubbery solid and eventually to liquid state. As the temperature increases, the additional thermal energy goes into the motion of larger segments of polymer chains, causing them to occupy a larger volume. [61]

The amorphous parts in semi-crystalline polymers go through the same increase of specific volume as well. However, the change in specific volume due to crystallization is of much greater significance. Figure 6 demonstrates schematically the correlation between temperature and specific volume for amorphous and semi-crystalline polymers on an arbitrary scale. Below the melting temperature, the morphology of semi-crystalline polymers consists of crystalline spherulites surrounded by amorphous phase. The spherulites consist of ribbon-like, folded polymer chains radiating outward from the central nucleation site. These lamellar chain-folded crystallites are separated by channels of amorphous material. The packing of polymer chains in crystalline regions is more efficient than in amorphous parts, which shows as a large change in specific volume at melting temperature. [61] This crystallization related variation in specific volume differentiates the semi-crystalline polymers from completely amorphous counterparts, and is detrimental for dimensional stability of manufactured articles.

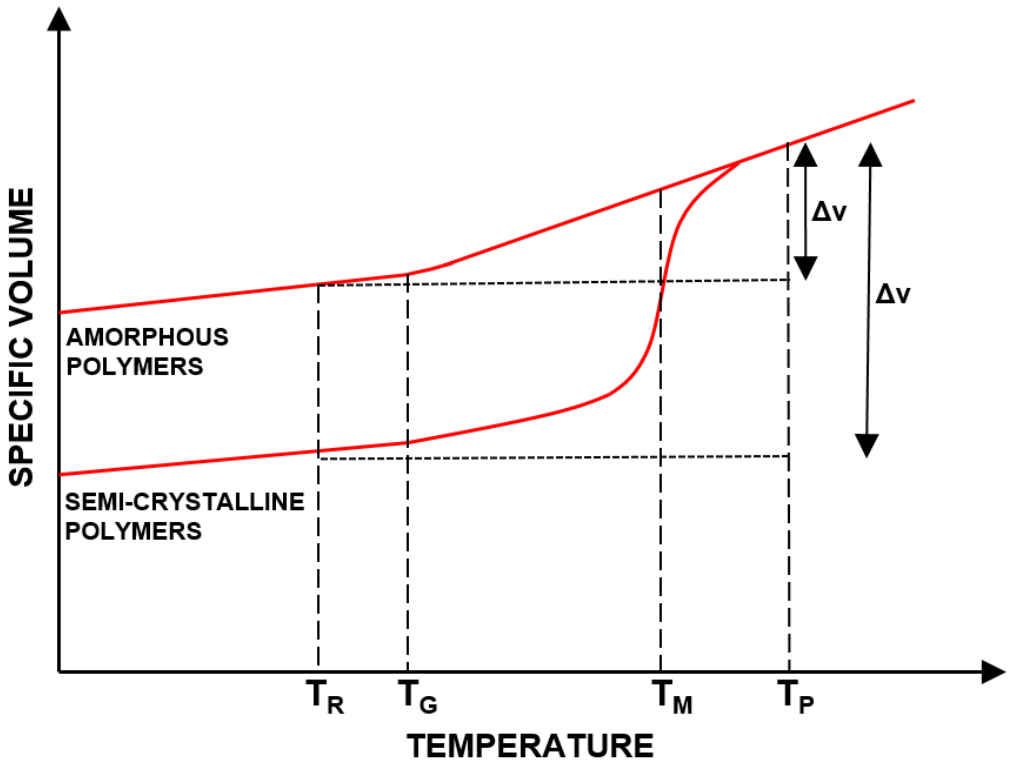

Figure 6. *Specific volume of semi-crystalline and amorphous polymers as a function of temperature. Semi-crystalline polymers display a substantial change in specific volume between processing temperature (T_p) and room temperature (T_r).*

The extent and characteristics of shrinkage of semi-crystalline polymers are a function of both intrinsic material properties and processing conditions. The main material properties affecting the shrinkage are degree of crystallinity and crystallization rate. The degree of crystallinity is essentially dependent on the tacticity of a polymer, and ranges from 10% to 80%, depending on the molecular characteristics [73]. The inherent degree of crystallinity of isotactic polyolefins lies in the upper end of the spectrum, causing substantial shrinkage due to the majority of the expanded molten material arranging into a high-density crystalline structure upon cooling. The shrinkage of semi-crystalline polymers is also dependent on the crystallization rate, i.e. the kinetics of nucleation and growth rate of crystals upon cooling [74]. The slower the crystallization rate, the lower is the crystalline content in the morphology directly after processing. If equilibrium degree of crystallinity is not attained during processing due to low crystallization rate, semi-crystalline polymers continue to gradually increase their crystalline percent towards equilibrium level, even at room temperature. This post shrinkage can take up to several weeks at room temperature before the processed part reaches its final stability [75].

From a processing point of view, there are several factors affecting the shrinkage characteristics of semi-crystalline polymers. On a general level, the most significant variables having an impact on the shrinkage are cooling conditions during deposition and other

factors that indirectly affect the cooling rate of deposited plastic. Some processing methods can also introduce additional parameters to control the shrinkage, such as injection and holding pressures in injection molding. However, in fused deposition modeling based methods the control of shrinkage is practically limited to the variables related to the cooling characteristics of deposited plastic.

A profound influence of cooling rate on the crystallization temperature and the final specific volume after cooling has been established in many past studies [76-78]. High cooling rate suppresses the crystallization process and shifts the crystallization onset temperature towards lower temperatures. The suppression of crystallization yields low degree of crystallinity and correspondingly higher percentage of amorphous portion in the morphology. Consequently, the specific volume of cooled down plastic increases with increasing cooling rate. Figure 7 demonstrates the dependence of specific volume on the cooling rate of semi-crystalline plastic. Besides shifting towards lower temperatures, the onset of crystallization spreads over a larger temperature range as the crystallization takes place at non-equilibrium conditions.

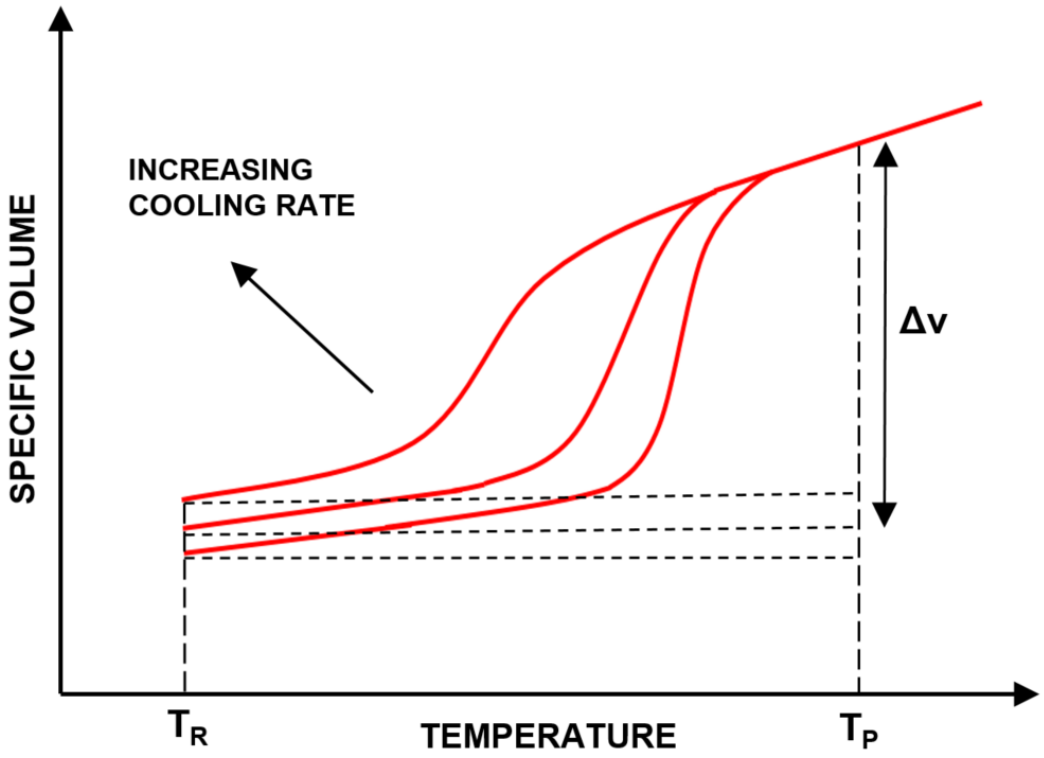

Figure 7. *The effect of cooling rate on the specific volume of semi-crystalline polymers.*

In fused deposition modeling, the cooling characteristics of the deposited filament are influenced by extrusion temperature, deposition environment temperature, and model cross section area. The higher the melt temperature at the time of extrusion, the longer it takes the plastic to cool down to build environment temperature. Additional heating elements, e.g., heated build platform and build chamber increase the build environment temperature, lowering the cooling rate and thus promoting the development of crystalline

morphology. By contrast, additional cooling during deposition suppresses the crystallization and can lead to parts with metastable morphology with higher specific volume. The amount of time spent on one layer also contributes to the cooling characteristics. Small cross sections are completed faster than large cross sections, assuming that print head speed remains constant. The shorter the time to complete a full layer, the shorter is the time for cooling before a subsequent layer is deposited above. Consequently, the average temperature of parts with small cross section remains higher during the deposition, lowering the overall cooling rate of the part and increasing the degree of crystallinity.

3.3.2 Warp deformation in FDM process

The shrinkage of feedstock materials during FDM process remains a significant source of dimensional error. However, the pure shrinkage alone does not account for the total dimensional inaccuracy. Volumetric shrinkage in combination with thermal gradients gives rise to thermal warping, as residual stresses build up in the deposited article. Warping can be described as unsolicited distortions in article's shape when compared to original model. Polymers that show high volumetric shrinkage upon cooling are especially prone to warping and consequently suffer from severe dimensional instability in FDM. [79-81]

Residual stress build-up in FDM arises from the solidification shrinkage induced contractile forces, as the plastic at liquefier temperature leaving the nozzle lands on the build surface or previously deposited plastic at lower temperature. Lower temperature surface freezes the contacting molten plastic in place and acts as a constraint for the shrinkage. Because an interfacial bond exists between the two layers, a contractile stress develops at the interface as the still molten plastic above the interface continues to shrink while cooling down. Figure 8 demonstrates how the residual stresses can cause warp deformation in the deposited articles. Right after the deposition of the second layer, no stresses have yet formed on the interface since the low viscosity solidifying plastic can accommodate the contractile forces. If sufficient interfacial bonding between the two layers and the build surface exists, the two layers show no warping but interlayer stresses develop as the uppermost layer continues to cools down. If, however, the interfacial bonding is insufficient, layers can detach from the build platform or delaminate from other layers due to the excessive stress build-up. The partial detachment of the object from the platform relieves some of the accumulated internal stresses, but impairs the aesthetics and functionality of the finished object. Severe or complete detachment of an object from the build platform and interlayer delamination are common occurrence for polymers with high tendency to shrink, and may lead to entirely failed deposition.

Warp deformation can also arise from differential cooling rates within the object. Varying cooling rates give rise to differences in shrinking characteristics and can lead to deviation from the original model dimensions. Plastics are poor heat conductors and part features with high thickness show decreased cooling rates compared to thin features [75]. This

part geometry related variation in cooling rate can cause warp deformation and is encountered in many plastic article manufacturing methods.

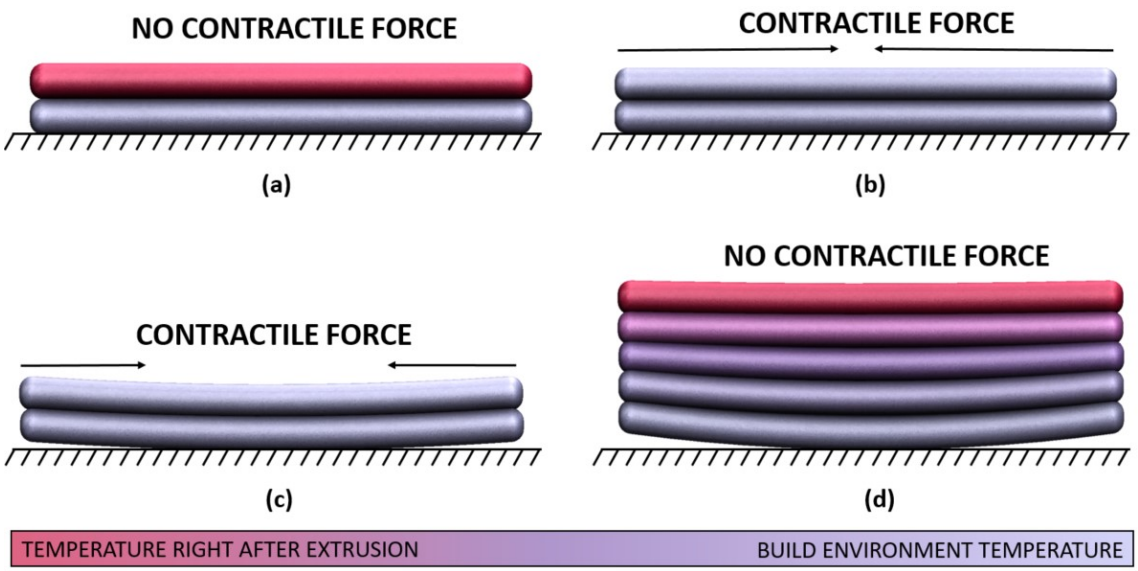

Figure 8. *Residual stress development and warp deformation right after the deposition of second layer (a), after cooling with sufficient (b) and insufficient (c) bonding to build platform, and after the deposition of fifth layer with insufficient bonding. After the cooling, contractile stresses are always present in the uppermost layer. Warping relieves the accumulated contractile stresses, but severely impairs the aesthetics and functionality of finished object.*

As previously has been established, the degree of crystallization of semi-crystalline polymers is influenced by cooling characteristics during processing. High cooling rates during processing can lead to suppressed non-equilibrium crystallization, and thus significant amount of post build shrinking. The residual stress build-up in FDM can lead to substantial warp deformation after the processing, especially when subjecting articles to elevated temperatures. By minimizing the stress build-up during processing, the post build warp deformation is also minimized. Therefore, heated build envelopes have traditionally been used to increase the temperature of already deposited plastic, making it more pliable and capable of accommodating the developing stresses. Lower cooling rates also allow higher degree of crystallization during processing, making articles less susceptible to post build warp deformation.

3.4 Current state of FDM of polyolefins

At the time of writing, very little research has been done to evaluate the performance of polyolefins as feedstock materials in FDM. Amorphous feedstock materials, such as ABS, are dominating the FDM industry, and it is only expected that most of the research focuses on these materials. Nonetheless, polyolefins have recently gained some interest as feedstock materials in FDM due to their attractive balance properties. The current state of

polyolefins in FDM is essentially still on research and development level, although a few commercial polyolefin-based filaments are already available.

Most of the recent research has been focused on polypropylene. Carneiro *et al.* [2] manufactured filament from extrusion grade and glass fiber reinforced polypropylene, and studied the effect of orientation, layer thickness and infill degree on the tensile properties of printed samples. Depending on the printing parameters, a 20-30% loss in the mechanical properties was observed when compared to compression molded counterparts. Hertle *et al.* [3] studied the bond formation of polypropylene in FDM by conducting shear tests to specimens deposited at different extrusion, substrate and cooling system temperatures. The most important factors affecting the bond formation were found to be the extrusion temperature and the temperature of already deposited layer. Kitson *et al. [4]* successfully used polypropylene as feedstock material in FDM to fabricate chemically resistant reactionware. Wang *et al. [72]* studied the effects of layer height and extrusion temperature on the formation of internal voids and Izod impact strength of deposited samples. A decrease in layer height lead to lower cell density and higher overall density of deposited sample. However, an increase in extrusion temperature lead to reduced impact strength. This was explained by the increased formation of β-crystals at lower temperatures, which improved the impact strength of PP. In three out of four studies, a PP plate was used as a build platform to improve the adhesion of the first layer and prevent the object from detaching during deposition.

Little to no research has been done concerning the FDM of polyethylene. Ramli *et al.* [82] prepared bio-compatible ultra-high-molecular-weight polyethylene (UHMWPE) filament for FDM purposes, but no further experimentation with PE-based filaments has been documented to date.

Despite of prior research, no comprehensive performance evaluation has been completed for polypropylene or polyethylene as feedstock materials in FDM. The experimental section in this work tries to supplement the previous studies and act as base for further studies in the area.

4. EXPERIMENTAL METHODOLOGY

In the experimental section of this thesis, the feasibility of two polyolefin materials as feedstock in FDM process was evaluated. The entire manufacturing chain, starting from filament preparation from pellets all the way through the final deposition, was controlled. Performance of these materials in FDM was assessed through depositing various test pieces and some results were compared with injection molded counterparts. The experimental methodology, from the filament fabrication to deposition process, will be discussed in following chapters.

4.1 Preparation of polyolefin filaments

4.1.1 Selected materials

For this study, semi-crystalline thermoplastic polypropylene and polyethylene were chosen as feedstock materials. Both materials are commercially available molding grade polyolefins, and were received in a form of pellets. The polypropylene is a heterophasic copolymer, characterized by high stiffness and impact strength. Typical uses for this grade are various molded items, such as automotive interior parts, crates and pails. The polyethylene is a high-density polyethylene, characterized by excellent impact strength and toughness. This polyethylene grade is also used for molded items, such as waste bins, crates and transport packaging. Table 4 summarizes the key properties and processing parameters for both materials. Data is provided by the manufacturer.

Table 4. *Key properties and processing parameters for the selected materials.*

Property	PP	PE	Standard
Density	0.905 g/cm^3	0.954 g/cm^3	ISO 1183
Melt Flow Index	20g/10min (230°C/2,16kg)	4g/10min (190°C/2,16kg)	ISO 1133
Tensile stress (At yield)	27 MPa	24 MPa	ISO 527-2
Processing Temperature	210-260 °C	210-275 °C	-
Molding shrinkage	1-2%	1-2%	-

For FDM purposes, the processing temperature and melt flow index of both materials are at feasible level, and comparable with current feedstock materials. However, the highly crystalline nature of the selected materials can lead to molding shrinkages up to 2%, which also is problematic for the dimensional stability in FDM process.

4.1.2 Filament preparation

The raw materials were supplied in the form of pellets, and they had to be prepared in to compatible filament with a diameter of 1,75 mm for further FDM purposes. This approach enabled the full control of the whole manufacturing chain and allowed a true comparison between printed and injection molded parts, as the same exact material was used in both cases.

Filament extrusion line consisted of a single screw extruder unit, an air cooling section and a pulling unit with foam rolls. A 4mm circular die was used, resulting into draw down ratio of approximately 5.2. Initially, water reservoir was used for cooling, but due to a formation of internal voids in the filament, pressurized air cooling was used instead. The air cooling section had a length of 500 mm and was positioned at a roughly equal distance from the extruder die. The finished filament freely coiled into a cardboard box, out of which it was later fed to the FDM machine. Apart from extrusion temperatures, same parameter values were used for both materials. Table 5 summarizes the detailed processing conditions for each material.

Table 5. *Summary of the key processing parameters for the filament fabrication.*

Parameter	PP	PE
Extruder zone temperatures (°C)	200/210/210	200/200/200
Die temperature (°C)	230	220
Extruder screw speed (RPM)	13	13
Pulling unit speed (m/min)	3.9	3.9
Cooling section length (m)	0.5	0.5

Several filament extrusion trials were needed to obtain the desired filament diameter and cross section. Due to partially insufficient cooling prior to pulling, the foam wheels of the pulling unit slightly flattened the warm and still malleable filament, leading to very slightly elliptic cross section with maximum and minimum diameters of 1,75 and 1,6; respectively. However, the maximum and minimum diameters of the cross section were consistent along the extruded filament, giving a precisely constant volume per unit volume of the filament.

4.2 Deposition methodology

4.2.1 Deposition setup

The 3D printer used for the deposition was a desktop model, based on a gantry style open-source Prusa i3 design. This exact model (GEEETech Prusa i3 M201) had a Bowden style dual extruder setup with a mixing liquefier, although only single extruder was used for

the testing purposes. All deposition tests were conducted using the 0.4 mm brass nozzle supplied with the printer. The printer was equipped with a liquefier capable of 240°C and heated build platform capable of 110°C. The factor limiting the upper extrusion temperature is the thermal softening polytetrafluroethylene (PTFE) tubing in the heat break above the nozzle. The purpose of the PTFE tubing is to facilitate the movement of softened feedstock material in the transition zone from solid to melt. Prolonged extrusion at temperatures above 240 °C can soften the tubing to the point at which it deforms and blocks the whole liquefier assembly and causes the deposition to fail.

The build platform consisted of a heated printed circuit board (PCB) with embedded resistor, layered with 3mm aluminum plate. Based on the initial testing with the prepared filaments and prior research [2, 4, 72], 5mm thick plates of matching polyolefin material were clamped above the heated build platform assembly to improve the adhesion. Both PP and PE showed very poor adhesion to traditional build platform materials, including glass, heat resistant Kapton tape and various adhesives.

A heated build environment was built for the printer to accurately control the ambient atmosphere during printing. With two relay controlled heating elements, the chamber was able to reach 50 °C. A DHT22 sensor was used to monitor and control the temperature, as well as to get humidity readings during printing. Temperature reading accuracy of ±0,5 °C was provided by manufacturer.

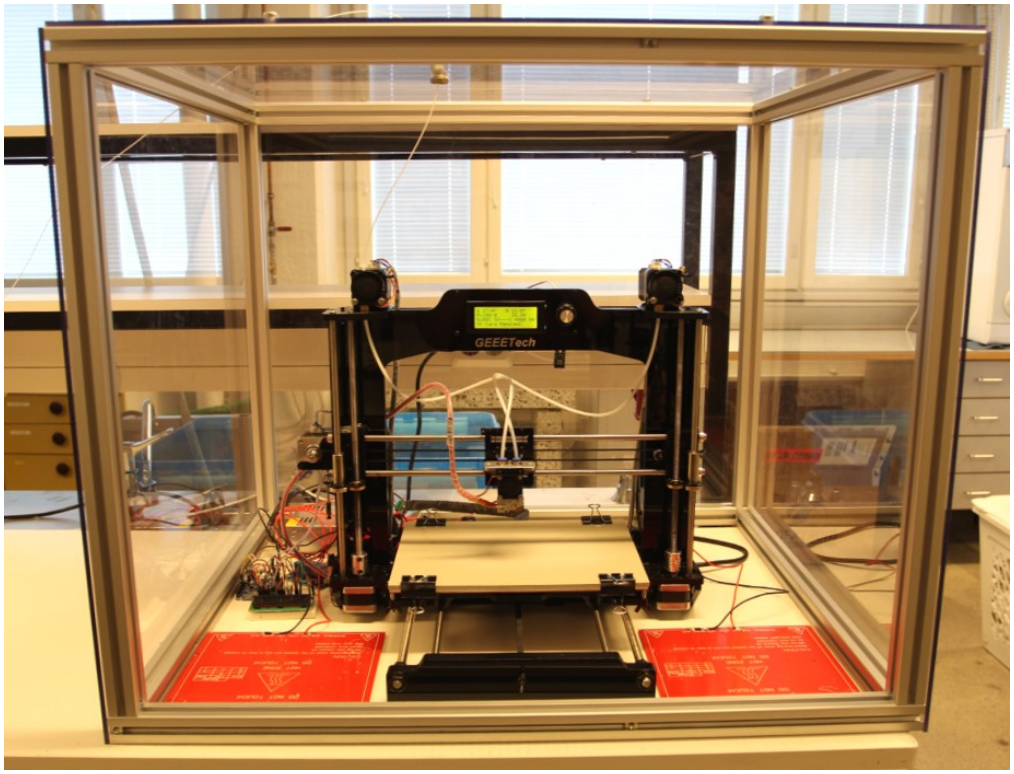

Figure 9. *The gantry style desktop 3D printer used in the study. The entire printer assembly was placed in heated build chamber for more refined control of the atmosphere during deposition.*

The extruded PP and PE filaments were fed to the printer straight from the cardboard boxes they were extruded in to. A dust filter was prepared and placed before the extruder to prevent any impurities from getting to the liquefier and interfering with the results.

Two pieces of FDM software were used for the deposition. Repetier-Host 2.01 was used to establish a connection between the printer and computer, and manually control the features of the printer. An open-source Slic3r Prusa Edition 1.34.1 slicing software was used to generate the path for the extruder, which was fed to the printer through the host software.

4.2.2 Selection of process variables

Since little to no information about depositing polyolefin materials was available, the starting points for operation specific printing parameters were defined by initial test prints. Furthermore, the temperature related parameters used in prior research showed significant variation depending on the source, and no clear consensus of optimum parameters was available. To evaluate the performance of these materials in FDM, the extrusion temperature, build platform temperature and build chamber temperature were selected as process variables.

The feasible extrusion temperature range was defined by manually extruding both materials in filament form at different temperatures from 150 °C to upwards in 10 °C increments. A 3 mm/s manual extrusion speed was used for the testing, representing a sufficient volumetric extrusion flow rate for the 0.4mm nozzle. Below 170 °C, the heat flux from the liquefier was insufficient to reliably melt either material at adequate rate, causing the extruder motor to fail to feed the filament. The upper extrusion temperature was limited by the PTFE tubing in the heat break. Thus, a value of 230 °C was chosen to avoid problems with the excessive softening of the tubing. Initial testing also indicated that extrusion temperature of 170 °C was too low to ensure sufficient bonding between the first layer and the build platform at room temperature (22 °C), leading to premature detachment of objects from the platform.

The build platform temperature was selected as a process variable in order to evaluate the adhesion characteristics and control the cooling of the deposited material. According to the information provided by manufacturer, the maximum temperature for the heated build platform was 110 °C. However, after clamping on the additional 5mm thick PP/PE plates, a maximum temperature of 80°C was measured on the surface with a contact probe thermometer after 30 minutes of pre-heating. A pre-heating period of same length was also used before the deposition of specimens to ensure stabilized conditions.

For further control of the cooling characteristics, the build environment temperature was varied between room temperature (22 °C) and 40 °C of the heated chamber. A 30-minute pre-heating period was used to stabilize the conditions prior to deposition.

Print head speed of 30 mm/s was used for all the specimens to minimize the effects of mechanical construction of the printer, as too high speeds may yield unwanted artifacts in the deposited articles. Layer height was varied between 0.2 mm and 0.3 mm depending on the specimen. Extrusion rate was set to 103% to compensate the slightly undersized filament. A 45°crossed rectilinear infill and infill percentage of 100% was used for all specimens. All articles were deposited with 0.5 mm line width and 25% infill-perimeter overlap.

4.2.3 Selected test specimens

The purpose of the experimental section of this thesis was to evaluate the performance of the PP and PE as feedstock materials in the FDM process. The evaluation was carried out by designing and depositing specimens with a varying set of process parameters and comparing the results. The adhesion properties, self-bonding, shrinkage and warping characteristics were the main areas of interest and assessed with deposition tests described below.

The bonding characteristics of both filaments were investigated by preparing uniaxial tensile dog-bone specimens at different extrusion and atmospheric temperatures. An EN ISO 527-2 1BA tensile test specimen was chosen for its small size, allowing rapid preparation with the FDM machine (see Figure 10). For all tensile test specimens, a 0.2 mm layer height was used to give accurate control over the thickness. One perimeter was used to maximize the share of uniform infill, while maintaining good dimensional accuracy and surface quality. Five specimens were prepared with each set of temperature parameters, and in order to facilitate the preparation, all five specimens were deposited at once. Table 6 lists all the combinations of the temperature parameters. No specimens could be prepared at room temperature with an extruder temperature of 170 °C, without premature detachment from the build platform. Consequently, this set was omitted from the further consideration.

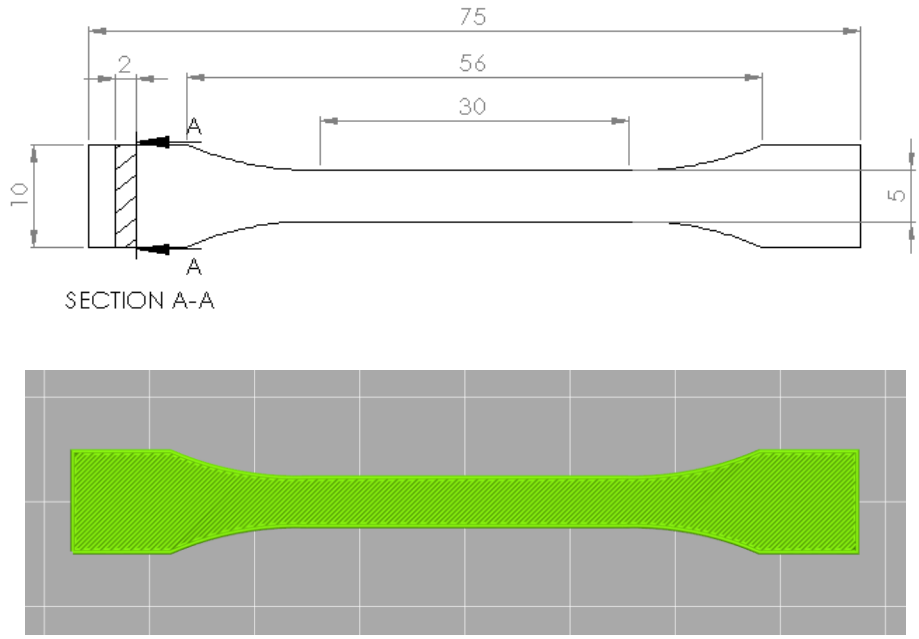

Figure 10. *An EN ISO 527-2 1BA tensile test specimen was used to evaluate the bonding at varying deposition conditions. 2D model with dimensions (top) and sliced model ready for deposition (bottom).*

Table 6. *Summary of the different temperature combinations used in the preparation of tensile test specimens. Similar sets from 1 to 5 were used for both materials.*

Set #	Extruder T (°C)	Platform T (°C)	Chamber T (°C)
Set 1	170	80	40
Set 2	200	RT	RT
Set 3	200	80	40
Set 4	230	RT	RT
Set 5	230	80	40

The shrinking and warping characteristics of the materials in the FDM process were evaluated using 20x20x20 mm solid cubes and 20 mm tall cylinders with equivalent volumes of 8 cm^3. Figure 11 shows the sliced models. The cooling conditions of deposited material were varied by altering the build platform temperature, build chamber temperature and deposition strategy. Using both materials, specimens were first deposited individually at 230 °C extruder temperature, while keeping build platform and build chamber at room temperature. Next, specimens were again individually deposited at 230 °C while having the build platform temperature at 80 °C and build chamber temperature at 40 °C. In the last experiment, both samples were deposited simultaneously, having the extruder, build platform and build chamber at 230 °C, 80 °C and 40 °C, respectively. By having the both specimens deposited at the same time, the cooling time between successive layers was doubled, lowering the average temperature of the specimen during building. Table 7 summarizes the combinations of deposition conditions used in the experiment.

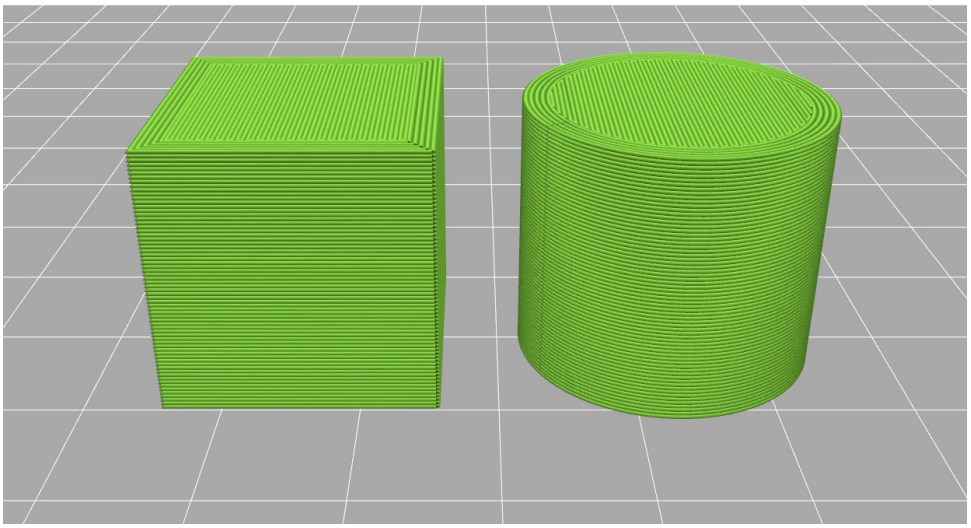

Figure 11. *A 20mm cube and a cylinder with equivalent volume were used to test the shrinking and warping characteristics of the PP and PE filaments.*

Table 7. *Summary of the deposition conditions used for the shrinking and warping evaluation. Simultaneously deposited specimens are tagged with an asterisk.*

Specimen	Extruder T (°C)	Platform T (°C)	Chamber T (°C)
Cube	230	RT	RT
Cube	230	80	40
Cube*	230	80	40
Cylinder	230	RT	RT
Cylinder	230	80	40
Cylinder*	230	80	40

The shrinking and warping characteristics of PP and PE feedstock materials in FDM process were further investigated by depositing specimens with thin features. Large-sized thin walled parts are especially prone to warping in FDM process and have thus remained as a significant challenge to date [83]. The susceptibility of PP and PE to warping in thin walled parts was assessed by depositing hollow cubic and cylindrical specimens with a 50 mm height and 1mm wall thickness. Figure 12 shows the sliced specimens. Using both materials, specimens were first deposited individually with 230 °C extruder temperature, while having the build platform and build chamber at room temperature. Next, the same specimens were deposited at 230 °C extruder temperature with build platform at 80 °C and build chamber at 40 °C.

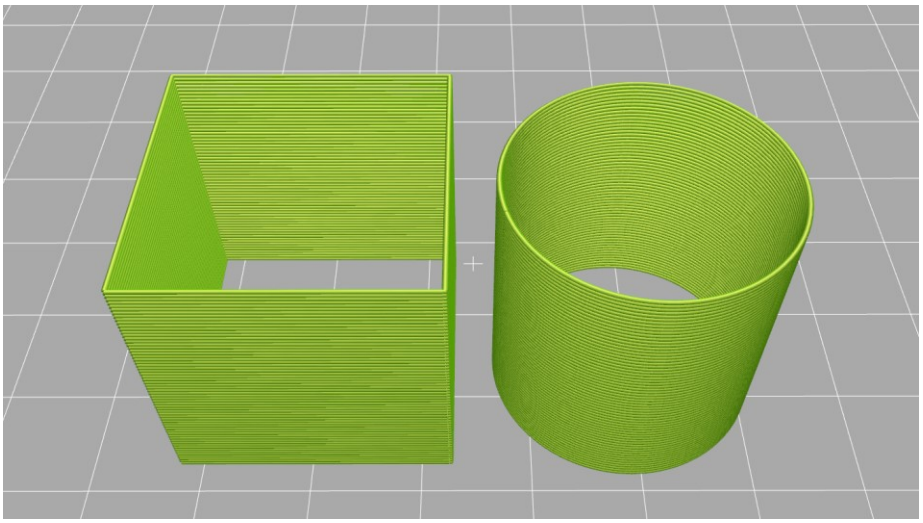

Figure 12. *Hollow cubic and cylindrical specimens with a wall thickness of 1mm were prepared to evaluate the warping characteristics of thin features.*

The final experiment to evaluate the deposition performance was a bridging test. In bridging, strands of filament are extruded in the middle of air with no supporting structures straight beneath. A set of specimens with varying bridge lengths was specifically designed for this purpose (see figure 13). All bridges were deposited 3 mm from the build platform between small support structures. The separation between support structures ranged from 20 mm to 100 mm. A bridge extrusion flow rate ratio of 0.9 was used to prevent sagging and first layers of the bridges were deposited with a print head speed of 10 mm/s. Bridging tests for both materials were carried out using 230 °C extrusion temperature, 80 °C build platform temperature and 40 °C build chamber temperature.

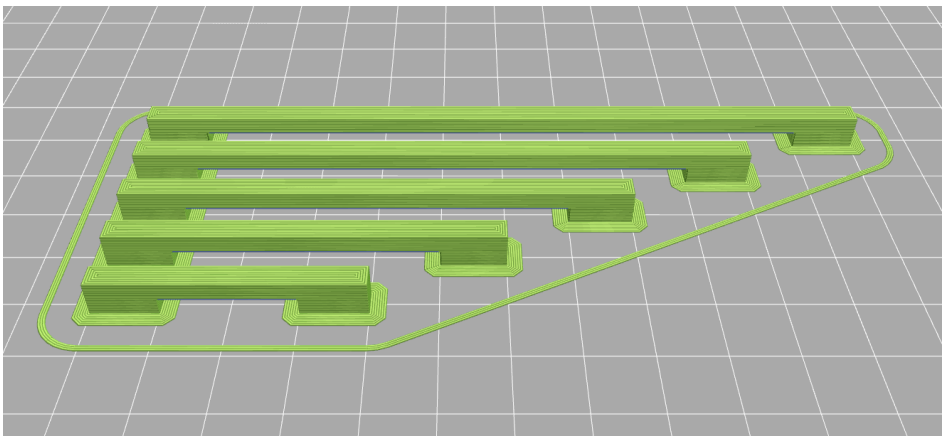

Figure 13. *The bridging properties of the PP and PE filaments were investigated with a specifically designed test pieces. Bridge lengths from 20mm to 100mm were tested with both materials.*

4.3 Preparation of injection molded samples

In order to obtain a comparable evaluation of the mechanical properties of printed samples, injection molded tensile test specimens were prepared from the same feedstock materials. The same uniaxial dog-bone tensile specimen, EN ISO 527-2 1BA, was chosen to get a true comparison between the printed and molded specimens.

Molding was carried out using a DSM Xplore micro twin-screw compounder and a DSM Xplore micro injection molding machine. Process parameters were set partly according to material manufacturers' suggestions and partly based on initial testing. Table 8 summarizes the key molding parameters for each material.

Table 8. *Summary of the key molding parameters used for each material.*

Parameter	PP	PE
Melt temperature (°C)	250	240
Mold temperature (°C)	30	40
Injection pressure (MPa)	4	4
Hold pressure (MPa)	4	4
Hold time (s)	6	6

After the establishment of the correct process parameters, five tensile specimens were prepared from each material. No post processing of the specimens was required as no flash or other molding artifacts appeared after optimizing the process.

4.4 Characterization of materials and specimens

The deposited and injection molded tensile specimens were tested with an Instron 5967 universal testing machine using a 2 kN load cell. Initial grip distance of 58 mm and 20 mm/s cross-head speed were used for all specimens. Tensile strength was calculated based on the tensile test data, and displacement data was used to evaluate the ductility of the deposited specimens.

The differential scanning calorimetry (DSC) testing was conducted using a NETZSCH DSC 204 F1 machine. A heating cycle from -20 °C to 220 °C and a cooling cycle from 220 °C to 20 °C with 10°C/min heating/cooling rate were used for both materials.

Optical microscopic analysis was performed for intact tensile test specimens to study the mesostructure resulting from differing processing conditions. Samples were prepared by cryogenically freezing a tensile test specimen and splitting it in half in a 90° angle.

5. RESULTS AND DISCUSSION

This section reviews the results from the experimental section. An overall performance analysis is provided to assess the feasibility of the polyolefin materials in FDM process, and suggestions for further research will be presented in the final chapter.

5.1 Effect of deposition conditions on bonding

To visualize the influence of the deposition conditions on the bonding of polymer roads, tensile tests were performed. In figure 14, the influence of extrusion temperature, build platform temperature and build chamber temperature on the yield stress is illustrated. For a comparison, the injection molded counterparts are included in the graph. Tensile test graphs representing typical tensile behavior of molded and FDM processed PP and PE are shown in figure 15.

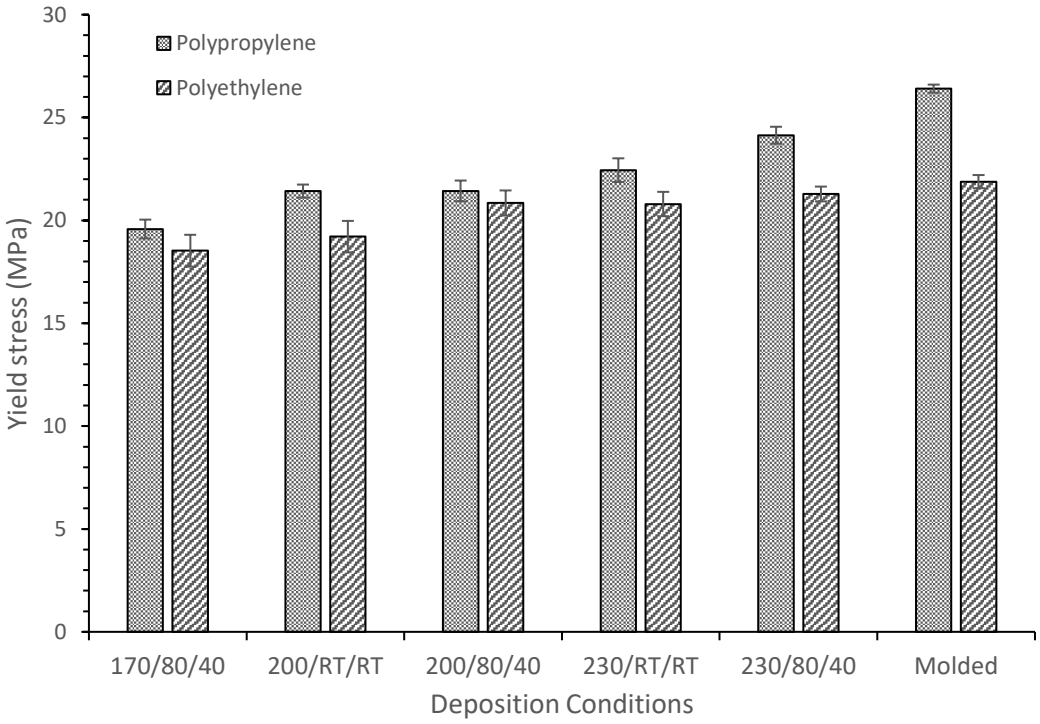

Figure 14. *Yield stresses for both materials at various deposition conditions. Extrusion temperature, build platform temperature and build chamber temperature are separated with slashes.*

For the FDM processed polypropylene, the maximum yield stress was reached with the extrusion, build platform and build chamber temperatures of 230 °C, 80 °C and 40 °C, respectively. The maximum yield stress of deposited specimens is approximately 90% of

the yield stress of the molded counterparts and the value provided by the manufacturer. Correspondingly, the 170 °C extrusion temperature and room temperature deposition conditions resulted into lowest yield stress. The lowest obtained yield stress value is roughly 70% of the yield stress of the molded specimens and manufacturer's data.

For the FDM processed polyethylene, the highest extrusion, build platform and build chamber temperatures resulted in the highest yield stress as well. However, the maximum yield stress is up to 95% of the yield stress of molded specimens and 88% of the manufacturer's reported value. Lowest yield stresses were once again reached with lowest deposition temperatures, amounting to 86% of the yield stress of the molded specimens and 77% of the value provided by manufacturer.

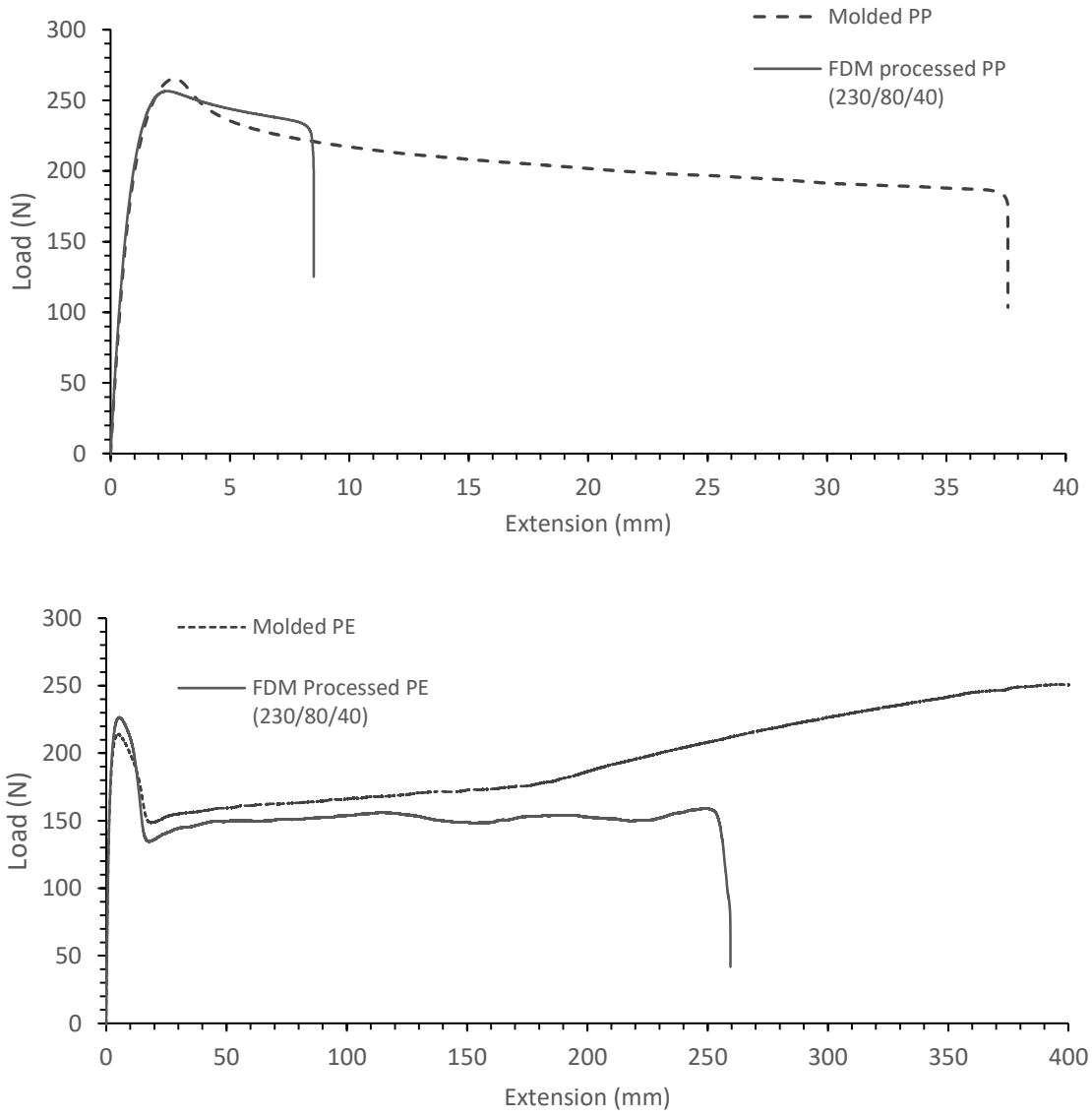

Figure 15. *Typical tensile test graphs for molded and FDM processed PP and PE. Even when deposited under optimal conditions, the necking of FDM processed PE was very uneven all the way up to the break.*

Above results are expected and in good agreement with theoretical considerations. The higher the extrusion temperature, the longer it takes the deposited polymer roads to cool down, allowing better neck growth and molecular diffusion between adjacent roads. Improved necking in turn reduces the size of the internal voids within the deposited part [26]. A similar effect is acquired by increasing the temperature of the build platform and build chamber. The additional heat from these heating elements slows down the cooling of the deposited polymer roads and keeps the average temperature of the part higher, leading to higher degree of necking. On the other hand, when the polymer is extruded on a cool substrate, whether it is the previous layer or the build platform, the time for neck formation is much shorter. Figure 16 shows the difference in internal mesostructure resulting from the optimal and worst deposition conditions for polypropylene. Ultimately, the combination of higher neck growth and increased molecular diffusion across the interface shows as an increase of yield stress during tensile testing.

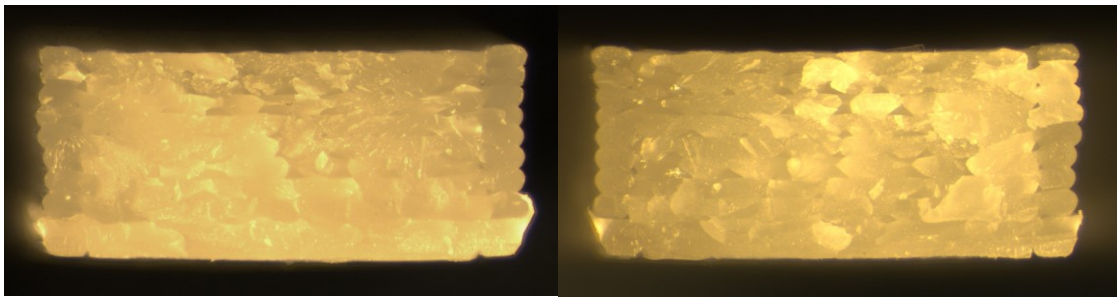

Figure 16. *The difference in the internal mesostructure of polypropylene specimens prior tensile testing. Mesostructures resulting from the best (left) and worst (right) deposition conditions.*

Based on the tensile tests, the difference in mechanical performance resulting from the optimal and worst deposition conditions is 20% for the PP and 13% for the PE. The reduced correlation of the yield strength of polyethylene with deposition conditions could be due to the difference in melting temperatures of the two materials. The DSC run revealed over 30 °C lower melting temperature of polyethylene, compared to the polypropylene feedstock (see Figure 17). This gives more time for necking between adjacent PE roads when deposited at the same temperature with the PP. PE could thus reach a maximum degree of necking at lower temperatures, diminishing the effect of temperature in the chosen temperature range.

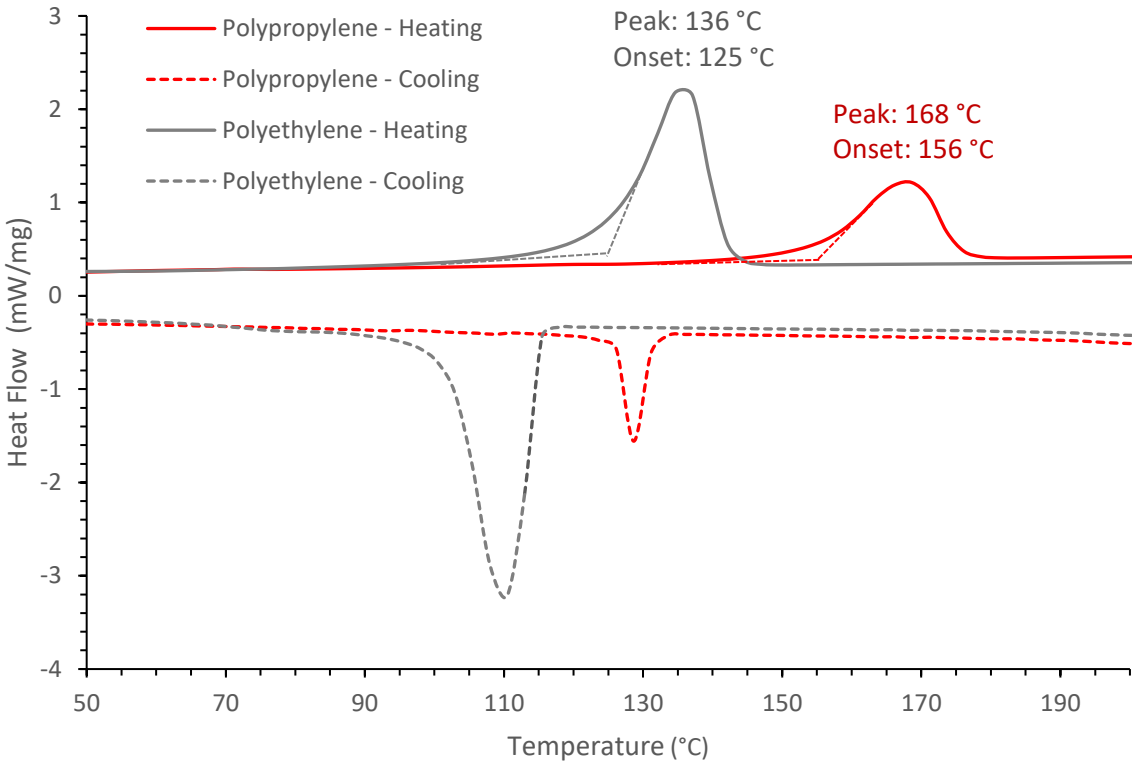

Figure 17. *DSC curves revealed a substantial difference in the melting temperatures of the crystalline portion between the PP and PE.*

Figure 18 shows the elongation of tensile specimens. For polypropylene, little to no correlation can be found between the deposition conditions and elongation. All specimens, regardless of deposition conditions, showed poor elongation and roughly 25% of the elongation of injection molded counterparts was reached. Similar results were obtained with polyethylene. Little consistency is found in the fracture characteristics of the deposited specimens. Some of the polyethylene specimens deposited under optimal conditions exhibited over 250 mm elongation, while most broke before 100 mm elongation. Generally, the deposited polyethylene specimens exhibited only a fraction of the elongation of injection molded counterparts, for which the test was stopped at 400 mm elongation.

However, the poor elongation results are expected, considering the layer-by-layer manufacturing method and 45° crossed infill deposition strategy. The voids and deposition instabilities within the mesostructure act as nucleation sites for fractures and cause premature breakdown of the specimens. The high amount of various inconsistencies within the specimens makes it difficult to accurately predict the ductility and fracture behavior of the deposited objects. To improve the ductility and its predictability, infill orientation needs to be aligned with the stress to minimize the tensile forces across the interface of polymer roads. However, such deposition strategy increases the anisotropy of mechanical properties compared to 45° crossed infill pattern, and may not be suitable for all applications.

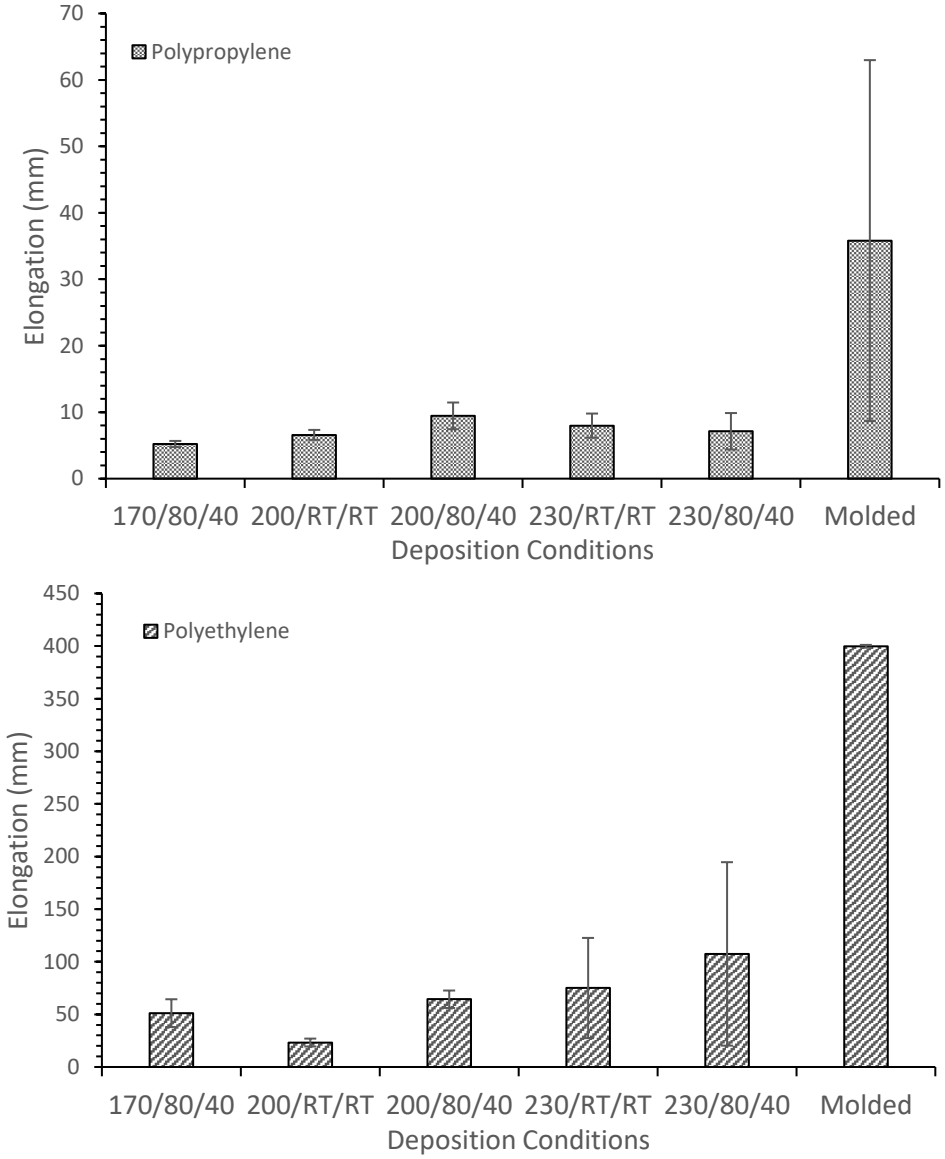

Figure 18. *Average elongation and standard deviation of deposited polypropylene (top) and polyethylene (bottom) specimens at various deposition conditions. Results show little to no correlation between the amount of elongation and deposition conditions.*

5.2 Shrinkage and warping characteristics

The results of the shrinkage and warping test are documented in Figures 19 to 23. Figure 19 shows the 20mm cubic specimens deposited under three different conditions. For polypropylene, the 230 °C extrusion temperature with room temperature build platform and build chamber resulted into a dimensionally stable specimen, apart from the warped bottom corners. Not even the highest extrusion temperature was sufficient to ensure adequate bonding between the first layer and the build platform at room temperature, allowing the built up residual stresses to detach the four corners of the cube from the platform. Raising

the build platform temperature to 80 °C and build chamber temperature to 40 °C increased the bond strength between the first layer and platform, and consequently the bottom of the part did not suffer from notable warp deformation. The additional heat flow from the heating elements also maintained the material more malleable, making it capable of accommodating the accumulating stresses arising from the shrinkage. However, the increased heat flow also decreased the cooling rate of the specimen during deposition. The core of the specimen remained at higher temperature throughout the deposition, leading to further crystallization than the outer regions subjected to more effective convective cooling. Consequently, all faces apart from the bottom one showed small indentations similar to sink marks encountered in many molding processes. Doubling the inter-layer cooling time resulted in the most dimensionally stable specimen and virtually no defects were apparent in the finished specimens. The heated platform ensured adequate bonding to the first layer, preventing the warping of the bottom layers. Due to doubled inter-layer cooling time, the average temperature of the deposited specimen remained lower and thus reduced the overall shrinkage.

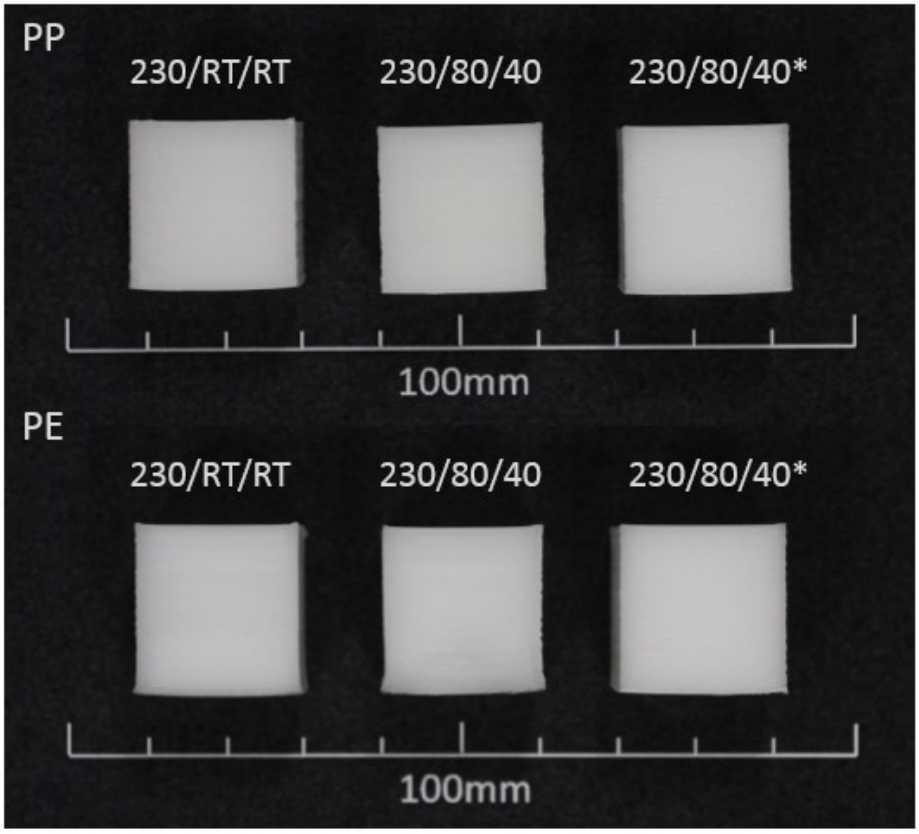

Figure 19. *Results from the cubic shrinking and warping tests. Simultaneously deposited specimens are marked with an asterisk.*

Polyethylene exhibited similar performance in the cubic shrinking test. However, in the case of 230 °C extrusion temperature, 80 °C build platform temperature and 40 °C build chamber temperature, the heat flow to the deposited specimen was so high that clear signs

of shrinkage were apparent. The specimen was severely deformed around the base and all open faces had deep shrinkage induced indentations. During the deposition, the core of the cubic PE specimen remained visibly translucent, whereas PP specimens turned more opaque prior the deposition of the successive layer. This can be attributed to the over 30 °C lower melting temperature of the PE. Essentially, the lower melting temperature allows further crystallization when deposited under similar conditions with PP, resulting into higher shrinkage.

The results of the cylindrical shrinkage test are shown in Figure 20. For both materials, the 230 °C extrusion temperature with no additional heating resulted in dimensionally stable specimens, apart from the slight warp deformation in the bottom layers. Enabling the heated build platform and build chamber resulted in virtually nonexistent warping in the bottom layers, but the specimens suffered from sink marks in the round top face. The PE specimens suffered from higher shrinkage than the PP counterparts, as was the case with cubic specimens. Doubling the cooling time resulted again in the most dimensionally stable specimens and no shrinkage induced defects were apparent.

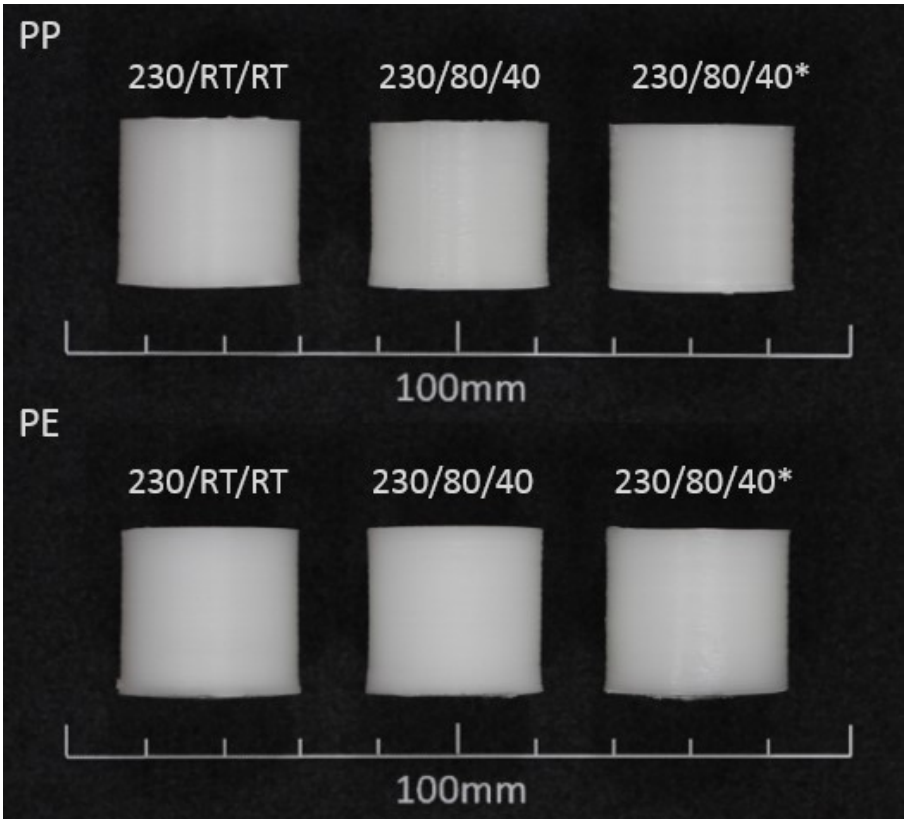

Figure 20. *Results from the cylindrical shrinking and warping tests. Simultaneously deposited specimens are marked with an asterisk.*

All around, the cylindrical specimens exhibited better dimensional stability than the cubic counterparts did, and the warp deformation in the bottom layers was clearly less than the deformation in cubic specimens deposited under same conditions. This can be explained

with the geometrical differences between the two specimens and how the stresses build up in them during the deposition. When a cubic specimen is deposited using the 45° crossed infill pattern, the lengthwise shrinkage of the polymer roads in the infill causes a contractile force from corner to corner within the layer. Additionally, the net force originating from shrinking perimeters is pointed towards the center at a 45° angle. Figure 21 illustrates the scenario for one corner of a cube. The stresses concentrate in the sharp corners of the cube, eventually overcoming the bonding strength to the build platform and peeling the corner off it. However, in the case of the cylinder, no such stress concentration takes place ass the contractile forces originating from shrinkage are evenly distributed within the volume. Therefore, the cylindrical specimens show generally lower tendency of detaching from the build platform.

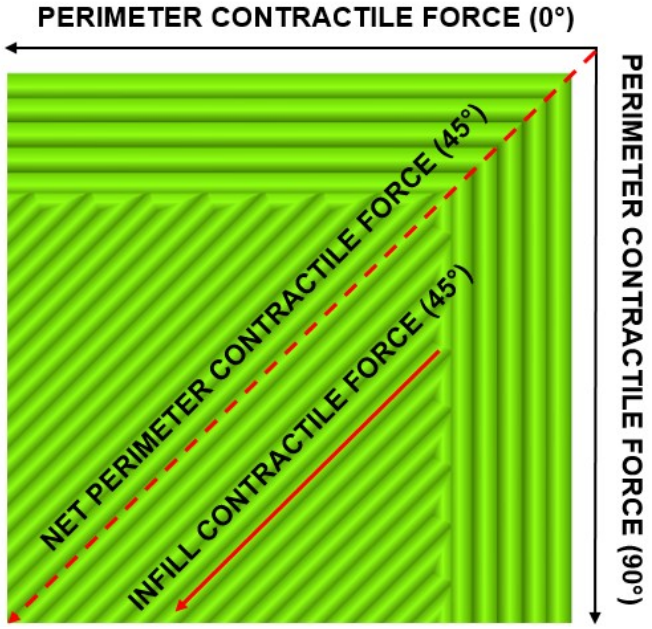

Figure 21. *Shrinkage induced contractile forces within a layer of a cubic specimen.*

The results of the thin wall warping tests are shown in figure 22. Both materials, regardless of the deposition conditions, displayed poor dimensional stability in the thin walled cubic specimen. Severe warp deformation is apparent in all four walls, and little to no resemblance to the digital analogue remains after the deposition. The cooling rate during deposition is so high in large thin walls that even the additional heat from the build platform or build chamber is not enough to help accommodate the developing stresses.

On the other hand, both materials performed significantly better when depositing the hollow cylindrical specimens. Yet again, the variation in performance can be attributed to the geometrical differences. In the hollow cubic specimens, the net contractile force in the perimeters points towards the center of the cube, as seen previously in Figure 21. When a certain amount of layers has been deposited, the concentrated stress build-up overcomes the bonding between the first layer and the build platform, peeling the corners

off the platform and distorting the rest of the deposition. However, the case of the hollow cylinder, the stress build-up is uniform due to the lack of sharp geometrical features. Consequently, the cylindrical specimens showed decreased warp deformation and remained completely attached to the build platform through the deposition.

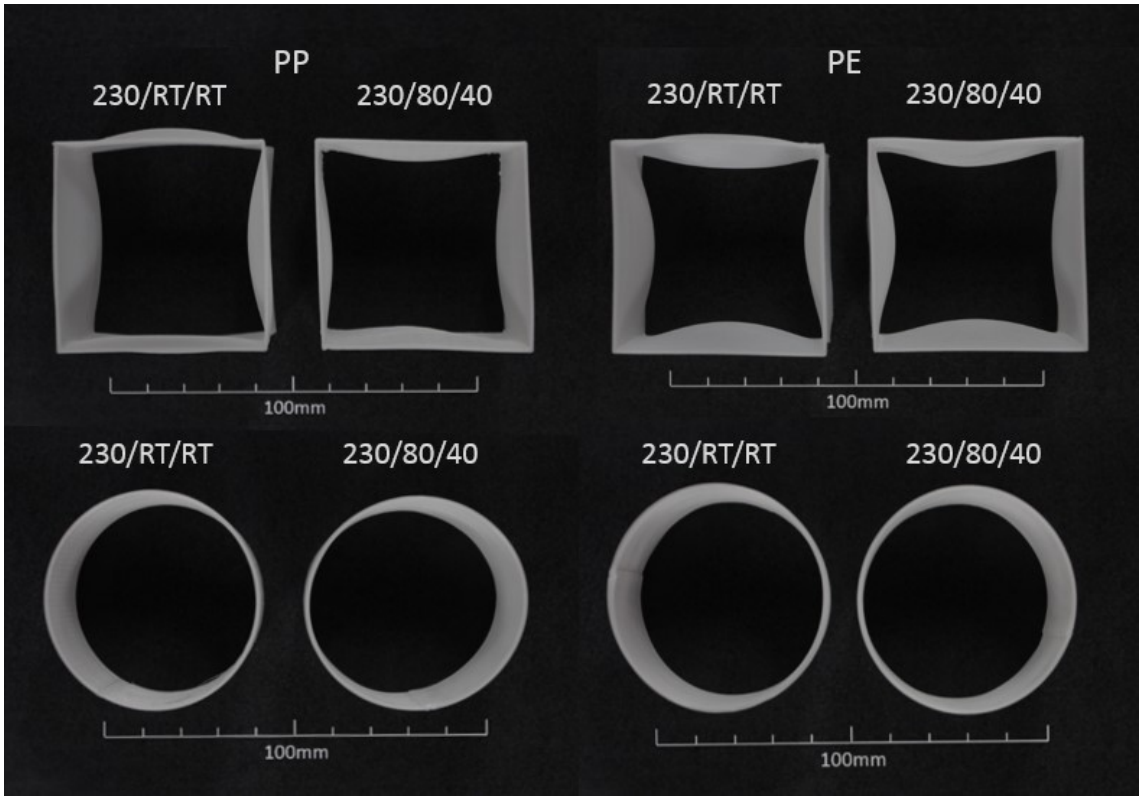

Figure 22. *Results from thin-feature warping test. Especially cubic specimens showed poor dimensional stability regardless of the deposition conditions.*

The results from the bridging tests are shown in figure 23. Both materials performed well, and apart from a few individual sagging filament strands, even the 100mm bridging test was a successfully completed. However, all bridging specimens show some degree of warp deformation with similar radii of curvature. This can be attributed to the specimens being removed from the build platform right after the deposition. After the detachment, the specimens remain at elevated temperature and crystallization proceeds. Because of the lack of constraints limiting the warping, i.e. the specimens are not anchored to the build platform, the specimens bend due to the contractile forces in the filament strands. Additionally, all filament strands within the bridged part were deposited lengthwise, amplifying the warp deformation. The few individual sagging filament strands can be attributed to the Bowden-style extruder setup. Due to the mechanical construction of the extruder, the built in pressure in the tubing releases quickly when the very first bridging stand is deposited in the middle of the air. This is supported by the fact that the diameter of the sagging strand is larger in the starting end of the bridge. Since the volumetric material flow is too high for the given print head speed, no tension is generated in the strand, and it sags from the horizontal deposition plane.

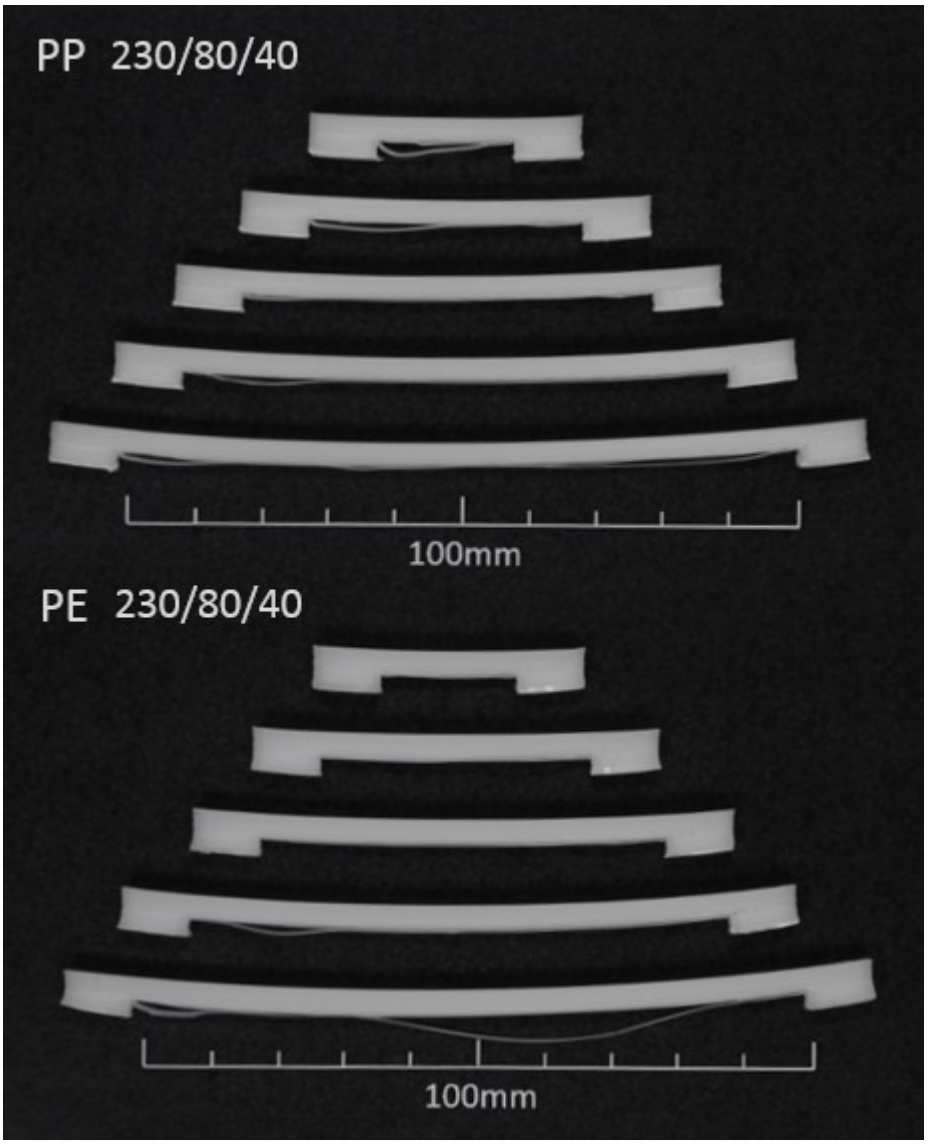

Figure 23. *Results from the bridging test.*

From a pure bridging performance standpoint, the high shrinkage of the PP and PE feedstock materials can be considered even a beneficial attribute. When an individual strand is deposited in the air at low speed, the shrinkage exerts a contractile force within the strand. The tension between the anchored part and the nozzle prevents the strand from sagging, aiding the bridging. When an adjacent strand is deposited next to the already deposited one, the shrinkage of the fresh strand further contracts the previously deposited strand, assuming that the two strands make a contact. Thus, the first layer of the bridge gradually lifts upwards and approaches the horizontal deposition plane, giving an adequate support for successive layers.

5.3 Overall performance analysis

Overall, the selected materials displayed mixed results in the fused deposition modeling process. While the FDM of molding grade semi-crystalline polyolefins is certainly possible, special arrangements and awareness of the challenges are required. Under optimal conditions, the deposition performance of the selected materials was for the most parts on par with many of the currently available feedstock materials. Moreover, only roughly 10% loss in yield strength was observed in deposited articles compared to injection molded counterparts. However, deviations from the optimal conditions impaired the dimensional stability and aesthetics of the deposited objects, or led to totally failed deposition.

The establishment of optimal conditions for the deposition is an intricate task, and the exact same set of deposition parameters may not yield best results in every case. Based on the tensile test results, the bonding of the deposited polymer is best at the highest deposition temperatures. From the pure bonding quality viewpoint, the extrusion temperature of 230 °C and the additional heat flow from the build platform and build chamber are thus advantageous for the adhesion between the first layer and build platform, interlayer bond strength, and overall mechanical properties. However, the deposition performance tests did indicate severe shrinkage when the cooling rate was excessively low. The high solidification shrinkage due to crystallization thus limits the total heat input that the deposited object can take without suffering from dimensional instability. Consequently, it is difficult to estimate the optimal deposition conditions, especially if a large variation in layer deposition times exists. Layers with small surface area have less time to cool down prior to the deposition of a successive layer, decreasing the overall cooling rate. On the other hand, layers with large surface area have more time to cool down before a new layer is deposited above, reducing the susceptibility for notable shrinkage.

While the deposition of thick features appears to be feasible, large thin features represent a significant challenge for the semi-crystalline polyolefins in fused deposition modeling. Thin walls (<1 mm) are especially prone to warping because of their weak mechanical structures and large contractile forces upon cooling [84]. The control over the warp deformation in such parts is very limited in FDM, limiting the feasible size of thin walls or constraining the process to higher wall thicknesses altogether.

5.4 Further research

While this work gives a basis for the fused deposition modeling of semi-crystalline polyolefins, there is still a lot room for further research. These materials show great potential as feedstock materials in FDM, but the inherently high solidification shrinkage limits the utilization on a grand scale. Thus, further research is needed to give a better control over the shrinking and warping behavior.

Mineral fillers have been observed to decrease the shrinkage and warp deformation of PLA in FDM process [39]. A 10% addition of talc or calcium carbonate halved the amount of warp deformation in a flat bar PLA specimen compared to neat PLA material. These additives represent attractive filler material choices for the semi-crystalline polyolefins, as they reduce the shrinkage, can have a reinforcing effect, and are non-abrasive [64]. Carneiro *et al.* [2] studied the effect of glass fibers on the tensile strength of fused deposition modeled polypropylene, but no effect on the shrinkage and warping behavior has been studied. The effect of these fillers on the printability should be thus assessed in the future.

Another promising method to improve the printability is to use dynamic local heating. Du *et al.* [83] studied the effect of local heating by laser irradiation on the tensile strength of ABS thin-walled parts. The moving laser spot increased local temperature, improving the material ductility and bonding quality. Consequently, almost a 200% increase in tensile strength was observed in the specimens with laser-assisted heating compared to ones deposited under normal conditions. The localized heating thus represents an attractive method to enhance the bonding quality and decrease the warping tendency of semi-crystalline polyolefins in FDM.

6. CONCLUSIONS

With the continuous developments in the field of fused deposition modeling technology, the method is no longer limited to rapid prototyping purposes only. As a technology, FDM has matured to the point where it is applied for various end-use applications and direct manufacturing of small product series. However, the range of materials is still limited, as many of the current feedstock materials are prone to degradation in harsh environmental conditions. This work evaluated the performance of PP and PE plastics as alternative feedstock materials in the FDM process. PP and PE are prevalent polyolefin plastics and their principal value lies in the attractive balance of physical properties in the solid state and chemical inertness. However, as semi-crystalline plastics, they suffer from substantial solidification shrinkage upon cooling, complicating the FDM process.

The approach used in this work allowed the full control over the entire manufacturing chain, from filament fabrication to deposition of specimens. The bonding quality was evaluated by preparing and testing tensile specimens, and comparing the results with injection molded counterparts. The overall deposition performance in the FDM process was assessed through preparing test specimens with varying geometries to evaluate shrinking and warping characteristics of the selected materials.

Tensile tests showed that the bonding of polymer stands was most efficient at the highest extrusion and build environment temperatures. Under these deposition conditions, only a 10% loss in yield strength was observed when compared to the injection molded counterparts. Correspondingly, the lowest extrusion and deposition environment temperatures resulted in 15-30% loss in the yield strength. In general, all specimens showed poor ductility and little to no correlation was found between the elongation and deposition conditions.

The deposition performance tests confirmed the underlying challenges of semi-crystalline polyolefin plastics in FDM. Under non-optimal deposition conditions, the combination of high solidification shrinkage and poor adhesion properties of polyolefins resulted in warp deformation and consequent partial detachment from the build platform. Low-temperature deposition conditions yielded dimensionally stable specimens, apart from the warped bottom faces. High-temperature conditions on the other hand resulted in clear signs of solidification shrinkage due to the decreased cooling rate. Excessive heat input caused large sink marks on flat faces but no warp deformation was apparent in the bottom face and specimens remained attached to the build platform. Doubling the interlayer cooling time under these conditions resulted in most dimensionally stable specimens, underlining the importance of optimal heat input and overall cooling rate of the specimen. Under optimal deposition conditions, the deposition performance of the PP and PE was for the most parts on par with many currently available feedstock materials.

The geometry of the part had also a profound effect on the warp deformation in the deposited specimens. Specimens with sharp elongated features in the bottom layers showed high tendency to peel off from the build platform due to the concentration of contractile stresses. The warp deformation in the bottom face was less apparent with circularly shaped specimens. In the case of large thin-walled (<1 mm) specimens with sharp corners, both materials displayed poor dimensional stability, and only little resemblance to the original digital model remained after the deposition. The weak mechanical construction of the thin walls and high contractile forces resulted in severe warp deformation, regardless of the deposition conditions. On the other hand, circular thin-walled specimens performed significantly better due to more uniform residual stress distribution.

All in all, the FDM of molding grade semi-crystalline polyolefins is certainly feasible, but special arrangements and awareness of the inherent challenges are required. Much of the error in dimensional accuracy of the final product arises from the shrinkage and warp deformation during the deposition process. In order to minimize the dimensional inaccuracies, the deposition conditions of semi-crystalline polyolefins need careful optimization. Further research in the area is still needed to bring the deposition performance closer to traditional filaments. Even so, as feedstock materials, they represent a unique option when toughness, low water absorption and high chemical resistance is required from the product. Feedstock materials with these attributes would make FDM technology applicable in even wider range of end-use applications in the future.

REFERENCES

[1] S.H. Masood, 10.04 - Advances in Fused Deposition Modeling, Comprehensive Materials Processing, Elsevier, Oxford, 2014, pp. 69-91

[2] O.S. Carneiro, A.F. Silva, R. Gomes, Fused deposition modeling with polypropylene, Materials & Design, Vol. 83, 2015, pp. 768-776

[3] S. Hertle, M. Drexler, D. Drummer, Additive Manufacturing of Poly (propylene) by Means of Melt Extrusion, Macromolecular Materials and Engineering, Vol. 301, Iss. 12, 2016, pp. 1482-1493

[4] P.J. Kitson, S. Glatzel, W. Chen, C. Lin, Y. Song, L. Cronin, 3D printing of versatile reactionware for chemical synthesis, Nature Protocols, Vol. 11, Iss. 5, 2016, pp. 920-936

[5] M. Kaveh, M. Badrossamay, E. Foroozmehr, A. Hemasian Etefagh, Optimization of the printing parameters affecting dimensional accuracy and internal cavity for HIPS material used in fused deposition modeling processes, Journal of Materials Processing Technology, Vol. 226, 2015, pp. 280-286

[6] D.G. Schniederjans, Adoption of 3D-printing technologies in manufacturing: A survey analysis, International Journal of Production Economics, Vol. 183, Part A, 2017, pp. 287-298

[7] S.S. Crump, Apparatus and method for creating three-dimensional objects, US, 5121329, US 07/429,012

[8] J.W. Stansbury, M.J. Idacavage, 3D printing with polymers: Challenges among expanding options and opportunities, Dental Materials, Vol. 32, Iss. 1, 2016, pp. 54-64

[9] R. Jones, P. Haufe, E. Sells, P. Iravani, V. Olliver, C. Palmer, A. Bowyer, RepRap–the replicating rapid prototyper, Robotica, Vol. 29, Iss. 01, 2011, pp. 177-191

[10] I. Gibson, D.W. Rosen, B. Stucker, Additive manufacturing technologies, 2nd ed. Springer, New York, 2010, 498 p.

[11] B. N. Turner, R. Strong, S. A. Gold, A review of melt extrusion additive manufacturing processes: I. Process design and modeling, Rapid Prototyping Journal, Vol. 20, Iss. 3, 2014, pp. 192-204

[12] S.H. Masood, Intelligent rapid prototyping with fused deposition modelling, Rapid Prototyping Journal, Vol. 2, Iss. 1, 1996, pp. 24-33

[13] S. Junk, C. Kuen, Review of Open Source and Freeware CAD Systems for Use with 3D-Printing, Procedia CIRP, Vol. 50, 2016, pp. 430-435

[14] D. Rypl, Z. Bittnar, Generation of computational surface meshes of STL models, Journal of Computational and Applied Mathematics, Vol. 192, Iss. 1, 2006, pp. 148-151

[15] R. Anitha, S. Arunachalam, P. Radhakrishnan, Critical parameters influencing the quality of prototypes in fused deposition modelling, Journal of Materials Processing Technology, Vol. 118, Iss. 1–3, 2001, pp. 385-388

[16] M.K. Agarwala, V.R. Jamalabad, N.A. Langrana, A. Safari, P.J. Whalen, S.C. Danforth, Structural quality of parts processed by fused deposition, Rapid Prototyping Journal, Vol. 2, Iss. 4, 1996, pp. 4-19

[17] M.E. Mackay, Z.R. Swain, C.R. Banbury, D.D. Phan, D.A. Edwards, The performance of the hot end in a plasticating 3D printer, Journal of Rheology, Vol. 61, Iss. 2, 2017, pp. 229-236

[18] G.S. Bual, Methods to improve surface finish of parts produced by fused deposition modeling, Manufacturing Science and Technology, Vol. 2, Iss. 3, 2014, pp. 51-55

[19] L.M. Galantucci, F. Lavecchia, G. Percoco, Experimental study aiming to enhance the surface finish of fused deposition modeled parts, CIRP Annals-Manufacturing Technology, Vol. 58, Iss. 1, 2009, pp. 189-192

[20] R. Singh, S. Singh, I.P. Singh, F. Fabbrocino, F. Fraternali, Investigation for surface finish improvement of FDM parts by vapor smoothing process, Composites Part B: Engineering, Vol. 111, 2017, pp. 228-234

[21] K. Jo, Y. Jeong, J. Lee, S. Lee, A study of post-processing methods for improving the tightness of a part fabricated by fused deposition modeling, International Journal of Precision Engineering and Manufacturing, Vol. 17, Iss. 11, 2016, pp. 1541-1546

[22] L.M. Galantucci, F. Lavecchia, G. Percoco, Quantitative analysis of a chemical treatment to reduce roughness of parts fabricated using fused deposition modeling, CIRP Annals-manufacturing technology, Vol. 59, Iss. 1, 2010, pp. 247-250

[23] S. Ahn, M. Montero, D. Odell, S. Roundy, P.K. Wright, Anisotropic material properties of fused deposition modeling ABS, Rapid prototyping journal, Vol. 8, Iss. 4, 2002, pp. 248-257

[24] A.R. Torrado, C.M. Shemelya, J.D. English, Y. Lin, R.B. Wicker, D.A. Roberson, Characterizing the effect of additives to ABS on the mechanical property anisotropy of specimens fabricated by material extrusion 3D printing, Additive Manufacturing, Vol. 6, 2015, pp. 16-29

[25] P. Chennakesava, Y.S. Narayan, Fused Deposition Modeling-Insights, Proceedings of the International Conference on Advances in Design and Manufacturing ICAD&M, Vol. 14, 2014, pp. 1345-1350

[26] Q. Sun, G.M. Rizvi, C.T. Bellehumeur, P. Gu, Effect of processing conditions on the bonding quality of FDM polymer filaments, Rapid Prototyping Journal, Vol. 14, Iss. 2, 2008, pp. 72-80

[27] J.F. Rodrıguez, Modeling the Mechanical Behavior of Fused Deposition Acrylonitrile-Butadiene-Styrene Polymer Components, Doctoral dissertation, University of Notre Dame, Dep.Aerosp.Mech.Eng., 1999

[28] J.P. Thomas, J.F. Rodrguez, Modeling the fracture strength between fused deposition extruded roads, pp. 16-23

[29] L. Li, P. Gu, Q. Sun, C. Bellehumeur, Modeling of bond formation in FDM process, The Transactions of NAMRI/SME, Vol. 31, 2003, pp. 613-620

[30] L Li, P. Gu, Q. Sun and C. Bellehumeur, Modeling of Bond Formation Between Polymer Filaments in the Fused Deposition Modeling Process, in: Journal of Manufacturing Processes, 2004, pp. 170-178

[31] L. Li, Q. Sun, C. Bellehumeur, P. Gu, Investigation of bond formation in FDM process, pp. 1-8

[32] W. Han, M.A. Jafari, K. Seyed, Process speeding up via deposition planning in fused deposition-based layered manufacturing processes, Rapid Prototyping Journal, Vol. 9, Iss. 4, 2003, pp. 212-218

[33] A. Clausen, N. Aage, O. Sigmund, Exploiting Additive Manufacturing Infill in Topology Optimization for Improved Buckling Load, Engineering, Vol. 2, Iss. 2, 2016, pp. 250-257

[34] A.K. Sood, R.K. Ohdar, S.S. Mahapatra, Improving dimensional accuracy of fused deposition modelling processed part using grey Taguchi method, Materials & Design, Vol. 30, Iss. 10, 2009, pp. 4243-4252

[35] W. Cheng, J. Fuh, A. Nee, Y.S. Wong, H.T. Loh, T. Miyazawa, Multi-objective optimization of part-building orientation in stereolithography, Rapid Prototyping Journal, Vol. 1, Iss. 4, 1995, pp. 12-23

[36] S.H. Masood, W. Rattanawong, P. Iovenitti, Part build orientations based on volumetric error in fused deposition modelling, The International Journal of Advanced Manufacturing Technology, Vol. 16, Iss. 3, 2000, pp. 162-168

[37] P. Alexander, S. Allen, D. Dutta, Part orientation and build cost determination in layered manufacturing, Computer-Aided Design, Vol. 30, Iss. 5, 1998, pp. 343-356

[38] D. Frank, G. Fadel, Expert system-based selection of the preferred direction of build for rapid prototyping processes, Journal of Intelligent Manufacturing, Vol. 6, Iss. 5, 1995, pp. 339-345

[39] S.H. Kochesfahani, Improving PLA-based Material for FDM 3D-Printers Using Minerals (Principles and Method Development), Plastics Engineering, 2016, pp. 1598-1614

[40] J.F. Rodrguez, J.P. Thomas, J.E. Renaud, Mechanical behavior of acrylonitrile butadiene styrene (ABS) fused deposition materials. Experimental investigation, Rapid Prototyping Journal, Vol. 7, Iss. 3, 2001, pp. 148-158

[41] M. Dawoud, I. Taha, S.J. Ebeid, Mechanical behaviour of ABS: An experimental study using FDM and injection moulding techniques, Journal of Manufacturing Processes, Vol. 21, 2016, pp. 39-45

[42] S. Ahn, M. Montero, D. Odell, S. Roundy, P.K. Wright, Anisotropic material properties of fused deposition modeling ABS, Rapid prototyping journal, Vol. 8, Iss. 4, 2002, pp. 248-257

[43] R. Salinas, 3D Printing with RepRap Cookbook, Packt Publishing Ltd, 2014, 341 p.

[44] L. Novakova-Marcincinova, J. Novak-Marcincin, Applications of Rapid Prototyping Fused Deposition Modeling Materials, Annals of DAAAM for 2012 & Proceedings of the 23rd International DAAAM Symposium, 2012

[45] L. Turng, Y. Srithep, Annealing conditions for injection-molded poly (lactic acid), Society of Plastics Engineers (SPE), 2014

[46] R. Singh, S. Singh, Development of nylon based FDM filament for rapid tooling application, Journal of The Institution of Engineers (India): Series C, Vol. 95, Iss. 2, 2014, pp. 103-108

[47] S. Singh, R. Singh, Experimental investigations for use of nylon6 industrial waste as FDM feedstock filament for investment casting applications, NISCAIR-CSIR, 2016

[48] K. Szykiedans, W. Credo, D. Osiński, Selected Mechanical Properties of PETG 3-D Prints, Procedia Engineering, Vol. 177, 2017, pp. 455-461

[49] M. Kaveh, M. Badrossamay, E. Foroozmehr, A. Hemasian Etefagh, Optimization of the printing parameters affecting dimensional accuracy and internal cavity for HIPS material used in fused deposition modeling processes, Journal of Materials Processing Technology, Vol. 226, 2015, pp. 280-286

[50] O.A. Mohamed, S.H. Masood, J.L. Bhowmik, Experimental investigation of time-dependent mechanical properties of PC-ABS prototypes processed by FDM additive manufacturing process, Materials Letters, Vol. 193, 2017, pp. 58-62

[51] W. Zhong, F. Li, Z. Zhang, L. Song, Z. Li, Short fiber reinforced composites for fused deposition modeling, Materials Science and Engineering: A, Vol. 301, Iss. 2, 2001, pp. 125-130

[52] A. Bandyopadhyay, K. Das, J. Marusich, S. Onagoruwa, Application of fused deposition in controlled microstructure metal-ceramic composites, Rapid Prototyping Journal, Vol. 12, Iss. 3, 2006, pp. 121-128

[53] J. Corney, S.H. Masood, W.Q. Song, Thermal characteristics of a new metal/polymer material for FDM rapid prototyping process, Assembly Automation, Vol. 25, Iss. 4, 2005, pp. 309-315

[54] M. Nikzad, S.H. Masood, I. Sbarski, Thermo-mechanical properties of a highly filled polymeric composites for fused deposition modeling, Materials & Design, Vol. 32, Iss. 6, 2011, pp. 3448-3456

[55] C. Vasile, Handbook of polyolefins, CRC Press, 2nd ed., 2000, 1032 p.

[56] M. Al-Ali AlMa'adeed, I. Krupa, Polyolefin Compounds and Materials: Fundamentals and Industrial Applications, 1st ed. Springer International Publishing, 2016, 354 p

[57] H. Karian, Handbook of polypropylene and polypropylene composites, revised and expanded, CRC press, 2003, 576 p.

[58] E.P. Moore, Polypropylene handbook: polymerization, characterization, properties, processing, applications, Hanser, 1996, 419 p.

[59] A. Peacock, Handbook of polyethylene: structures: properties, and applications, CRC Press, 2000, 544 p.

[60] C. Vasile, M. Pascu, Practical guide to polyethylene, iSmithers Rapra Publishing, 2005, 176 p.

[61] W.D. Callister, D.G. Rethwisch, Materials science and engineering, John Wiley & Sons NY, 2011, 992 p.

[62] G. Wypych, Handbook of polymers, Elsevier, 2016, 712 p.

[63] R.B. Seymour, C.E. Carraher, Structure-property relationships in polymers, 1st ed. Plenum Press, New York, 1984, 246 p.

[64] M. Kutz, Applied plastics engineering handbook: processing and materials, William Andrew, 2011, 574 p.

[65] J. Safka, M. Ackermann, D. Martis, CHEMICAL RESISTANCE OF MATERIALS USED IN ADDITIVE MANUFACTURING, MM Science Journal, Vol. 2016, Iss. 6, 2016, pp. 1573-1578

[66] E. Kim, E. Kim, Y. Shin, Y. Shin, S. Ahn, S. Ahn, The effects of moisture and temperature on the mechanical properties of additive manufacturing components: fused deposition modeling, Rapid Prototyping Journal, Vol. 22, Iss. 6, 2016, pp. 887-894

[67] Halidi, Siti Nur Amalina Mohd, J. Abdullah, Moisture effects on the ABS used for fused deposition modeling rapid prototyping machine, IEEE, 2012, pp. 839-843

[68] M. Notomi, K. Kishimoto, T. Shibuya, T. Koizumi, Effects of moisture absorption on fracture behaviors of acrylonitrile-butadiene-styrene resin, Journal of Applied Polymer Science, Vol. 72, Iss. 3, 1999, pp. 435-442

[69] Material selection guide, Curbell Plastics, Inc., 2016, Available (accessed on 12.7.2017): https://www.curbellplastics.com/Research-Solutions/Technical-Resources/Technical-Resources/Plastic-Material-Selection-Guide

[70] Probst Thomas, bvse market report on plastics, Bonn, 2017, Available (accessed on 12.7.2017): http://www.bvse.de/

[71] F. Awaja, M. Gilbert, G. Kelly, B. Fox, P.J. Pigram, Adhesion of polymers, Progress in polymer science, Vol. 34, Iss. 9, 2009, pp. 948-968

[72] L. Wang, D.J. Gardner, Effect of fused layer modeling (FLM) processing parameters on impact strength of cellular polypropylene, Polymer, Vol. 113, 2017, pp. 74-80

[73] G.W. Ehrenstein, Polymeric materials: structure, properties, applications, Carl Hanser Verlag GmbH Co KG, 2012, 277 p.

[74] S. Andjelić, R.C. Scogna, Polymer crystallization rate challenges: the art of chemistry and processing, Journal of Applied Polymer Science, Vol. 132, Iss. 38, 2015

[75] J. Fischer, Handbook of molded part shrinkage and warpage, 2nd ed. William Andrew, 2012, 292 p.

[76] H. Zuidema, G.W.M. Peters, H.E.H. Meijer, Influence of cooling rate on pVT-data of semicrystalline polymers, Journal of Applied Polymer Science, Vol. 82, Iss. 5, 2001, pp. 1170-1186

[77] S. Chakravorty, PVT testing of polymers under industrial processing conditions, in: Polymer Testing, 2002, pp. 313-317

[78] Van der Beek, Maurice H E, G.W.M. Peters, H.E.H. Meijer, The Influence of Cooling Rate on the Specific Volume of Isotactic Poly(propylene) at Elevated Pressures, Macromolecular Materials and Engineering, Vol. 290, Iss. 5, 2005, pp. 443-455

[79] A.H. Nickel, D.M. Barnett, F.B. Prinz, Thermal stresses and deposition patterns in layered manufacturing, in: Materials Science and Engineering: A, 2001, pp. 59-64

[80] T. Wang, J. Xi, Y. Jin, A model research for prototype warp deformation in the FDM process, The International Journal of Advanced Manufacturing Technology, Vol. 33, Iss. 11, 2007, pp. 1087-1096

[81] V.A. Safronov, R.S. Khmyrov, D.V. Kotoban, A.V. Gusarov, Distortions and Residual Stresses at Layer-by-Layer Additive Manufacturing by Fusion, Journal of Manufacturing Science and Engineering, Vol. 139, Iss. 3, 2017

[82] M.S. Ramli, M.S. Wahab, M. Ahmad, A.S. Bala, FDM preparation of bio-compatible UHMWPE polymer for artificial implant, ARPN Journal of Engineering and Applied Sciences, Vol. 11, 2016, pp. 5474-5480

[83] J. Du, Z. Wei, X. Wang, J. Wang, Z. Chen, An improved fused deposition modeling process for forming large-size thin-walled parts, Journal of Materials Processing Technology, Vol. 234, 2016, pp. 332-341

[84] S. Nian, C. Wu, M. Huang, Warpage control of thin-walled injection molding using local mold temperatures, International Communications in Heat and Mass Transfer, Vol. 61, 2015, pp. 102-110